

FIG. 5. RFs have a lower affinity to Fc fragment of IgG than anti-Fc Ab. Competitive inhibition ELISA showing that synovium-derived RFs (SY1 and SY2) and PBMC-derived RFs (PBMC1 and PBMC2) have a lower affinity to the Fc fragment of IgG than anti-Fc Ab.

peripheral B cells (2, 18). After 48 h of treatment, the cells were incubated with [³H]thymidine for 16 h, and its incorporation was measured. As shown in Fig. 6, synovium-derived RFs alone efficiently induced B-cell activation, and the addition of CD40L had a synergistic effect. On the other hand, PBMC-derived RFs did not induce B-cell activation (data not

shown). Figure 6 also shows that anti-Fc and anti-Fab Abs were equally potent as B-cell activators.

We report here that RFs can stimulate EBV lytic replication and polyclonal B-cell activation. This finding is quite conceivable because anti-Fc Abs induce EBV and B-cell activation as efficiently as anti-Fab Abs do. Although the degree of EBV and B-cell activation by SY RFs was lower than that by the anti-Fc Ab, this can be attributed to the difference in the specificity and the affinity to the Fc fragment of IgG: i.e., SY1 RFs reacted with IgG3, SY2 RFs reacted with IgG1, and the affinity of SY RFs was ca. 100 times lower than that of anti-Fc Ab. The 1,000-fold-lower affinity of PBMC-derived RFs compared to that of anti-Fc Abs would explain why they could not induce EBV and B-cell activation. Cross-linking the RFs by anti-human IgM Abs did not increase their ability to activate EBV (data not shown). These results also indicate that the differences in affinity of the various RFs described here could account for the failure of some RF to activate B cells.

It has been reported that RFs derived from RA patients include monoreactive and polyreactive RFs (4). Monoreactive RFs bind with relatively high affinity and have specificity for the IgG Fc fragment, whereas polyreactive RFs bind to a number of different self (e.g., ssDNA, Ins, Tg, etc) and non-self (e.g., TT and bacterial lipopolysaccharide) antigens (26). Although the molecular basis of these cross-reactivities has not been conclusively answered (6), many studies indicate that the V_H and V_L gene segments of monoreactive high-affinity Abs harbor more somatic mutations than the V_H and V_L gene segments of polyreactive low-affinity Abs, which is close to unmutated "germ line" genes (22, 28, 40).

Although we tested 10 RF-positive sera from patients with RA, only two sera induced EBV activation (5 and 1%, respectively) (data not shown). Since RFs in sera are bound by serum IgG, they must have lower IgG-binding capabilities. Moreover, several reports demonstrated that RFs produced by rheumatoid synovial cells had greater reactivity to the IgG3 subclass, in contrast to serum RF, which had greater reactivity to the human IgG1 subclass (29). Further observations indicated that synovium-derived RFs had greater affinity than PBMC-derived RFs (3). Because the synovium is the central site of patholog-

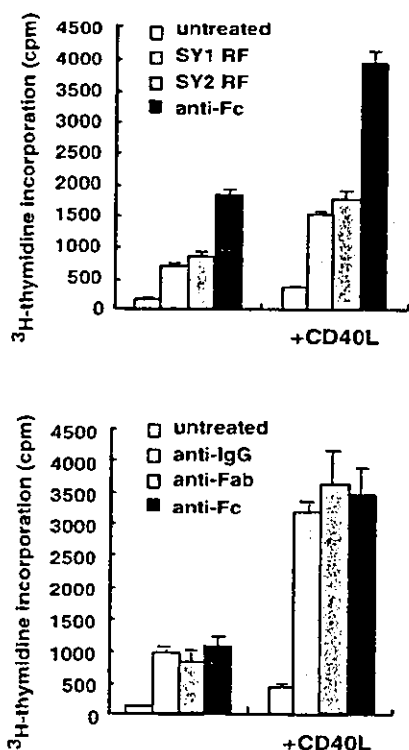


FIG. 6. RFs induce peripheral B-cell activation. Purified B cells (5×10^5) from adult peripheral blood were incubated with RFs (200 μ g/ml) and anti-IgG, anti-Fab, and anti-Fc Abs (50 μ g/ml) with or without the addition of CD40L (3 μ g/ml) for 48 h and then pulsed with 0.5 μ Ci of [³H]thymidine for 16 h. (Upper panel) Synovium-derived RFs, SY1 RF and SY2 RF, induce B-cell activation; (lower panel) anti-Fc Ab induces B-cell activation as efficiently as anti-Fab Ab.

ical activity in RA. RFs produced there may be pathogenically more important than RFs present in the intravascular space.

The present findings imply a possible role for RFs as EBV and B-cell activators. The role of EBV activation in the pathogenesis of RA remains to be clarified.

ACKNOWLEDGMENTS

We thank B. Sugden and T. Sculley for helpful discussions and critical reading of the manuscript and S. Tsuchida for technical assistance.

This study was supported by grants-in-aid from the Ministry of Education, Science, Culture, and Technology of Japan.

REFERENCES

- Alspangh, M. A., G. Henle, E. T. Lennette, and W. Henle. 1981. Elevated levels of antibodies to Epstein-Barr virus antigens in sera and synovial fluids of patients with rheumatoid arthritis. *J. Clin. Investig.* 67:1134-1140.
- Armitage, R. J., W. C. Fanslow, L. Strockbine, T. A. Sato, K. N. Clifford, B. M. Macduff, D. M. Anderson, S. D. Gimpel, T. Davis-Smith, C. R. Maliszewski, L. A. Clark, C. A. Smith, K. H. Grabstein, D. Cosman, and M. K. Spriggs. 1992. Molecular and biological characterization of a murine ligand for CD40. *Nature* 357:80-82.
- Burastero, S. E., P. Casali, R. L. Wilder, and A. L. Norkins. 1988. Monoreactive high affinity and polyreactive low affinity rheumatoid factors are produced by CD5⁺ B cells from patients with rheumatoid arthritis. *J. Exp. Med.* 168:1979-1992.
- Burastero, S. E., M. Cutolo, V. Dessi, and F. Celada. 1990. Monoreactive and polyreactive rheumatoid factors produced by in vitro Epstein-Barr virus-transformed peripheral blood and synovial B lymphocytes from rheumatoid arthritis patients. *Scand. J. Immunol.* 32:347-357.
- Carson, D. A., J. L. Pasquall, C. D. Tsoukas, S. Fong, S. F. Slovin, S. Lowrance, L. Strominger, and J. H. Vaughan. 1981. Physiology and pathology of rheumatoid factors. Springer Semin. Immunopathol. 4:164-179.
- Carayannopoulos, M. O., K. N. Potter, Y. Li, J. B. Natvig, and J. D. Capra. 2000. Evidence that human immunoglobulin M rheumatoid factors can be derived from the native antibody pool and undergo an antigen driven immune response in which somatically mutated rheumatoid factor have lower affinities for immunoglobulin G Fc than their germline counterparts. *Scand. J. Immunol.* 51:327-336.
- Catalano, M. A., D. A. Carson, S. F. Slovin, D. D. Richman, and J. H. Vaughan. 1979. Antibodies to Epstein-Barr virus-determined antigens in normal subjects and in patients with seropositive rheumatoid arthritis. *Proc. Natl. Acad. Sci. USA* 76:5825-5828.
- Chen, F., J. Zou, L. di Renzo, G. Winberg, L. Hu, E. Klein, G. Klein, and I. Eruberg. 1995. A subpopulation of normal B cells latently infected with Epstein-Barr virus resembles Burkitt lymphoma cells in expressing EBNA-1 but not EBNA-2 or LMP1. *J. Virol.* 69:3752-3758.
- Dobata, M., R. E. Humphreys, K. Takada, and T. Sairenji. 1980. Activation of latent EBV via anti-IgG-triggered, second messenger pathways in the Burkitt's lymphoma cell line Akata. *J. Immunol.* 144:4788-4793.
- DeFranco, A. L. 1997. The complexity of signaling pathways activated by the BCR. *Curr. Opin. Immunol.* 9:296-308.
- Ferrell, P. B., C. T. Aitchison, G. R. Pearson, and E. M. Tan. 1981. Seroprevalence study of relationships between Epstein-Barr virus and rheumatoid arthritis. *J. Clin. Investig.* 67:681-687.
- Hakoda, M., T. Ishimoto, S. Hayashimoto, K. Inoue, A. Taniguchi, N. Kamatani, and S. Kashiwazaki. 1993. Selective infiltration of B cells committed to the production of monoreactive rheumatoid factor in synovial tissue of patients with rheumatoid arthritis. *Clin. Immunol. Immunopathol.* 69:16-22.
- Hampar, B., J. G. Derge, L. M. Martos, and J. L. Walker. 1972. Synthesis of Epstein-Barr virus after activation of the viral genome in a "virus-negative" human lymphoblastoid cell (Raji) made resistant to 5-bromodeoxyuridine. *Proc. Natl. Acad. Sci. USA* 69:78-82.
- Jefferis, R., and R. A. Mageed. 1989. The specificity and reactivity of rheumatoid factors with human IgG. *Monogr. Allergy* 26:45-60.
- Kieff, E., and A. B. Rickinson. 2002. Epstein-Barr virus, p. 2579-2582. *In* B. N. Fields, D. M. Knipe, and P. M. Howley (ed.), *Fields virology*, 4th ed. Lippincott-Raven, Philadelphia, Pa.
- Konishi, K., S. Maruo, H. Kato, and K. Takada. 2001. Role of Epstein-Barr virus-encoded latent membrane protein 2A on virus-induced immortalization and virus activation. *J. Gen. Virol.* 82:1451-1456.
- Krause, A., T. Kamradt, and G. R. Burmester. 1996. Potential infectious agents in the induction of arthritides. *Curr. Opin. Rheumatol.* 8:203-209.
- Lahvis, G. P., and J. Cerny. 1997. Induction of germinal center B-cell markers in vitro by activated CD4⁺ T lymphocytes. *J. Immunol.* 159:1783-1793.
- Levo, Y., R. Fischel, and M. Ehrenfeld. 1981. Circulating immune complexes in patients with rheumatoid arthritis: correlation with disease activity. *J. Rheumatol.* 8:851-855.
- Luka, J., B. Kallin, and G. Klein. 1979. Induction of the Epstein-Barr virus (EBV) cycle in latently infected cells by *n*-butyrate. *Virology* 94:228-231.
- Mannik, M., F. A. Nardella, and E. H. Sasso. 1988. Rheumatoid arthritis. Springer Semin. Immunopathol. 10:115-277.
- Mark, J. S., C. W. Euler, S. C. Christensen, and J. William. 2003. Activation of rheumatoid factor (RF) B cells and somatic hypermutation outside of germinal centers in autoimmune-prone MRL *lpr* mice. *Ann. N. Y. Acad. Sci.* 987:38-50.
- Miller, C. L., J. H. Lee, E. Kieff, and R. Longnecker. 1994. An integral membrane protein (LMP2) blocks reactivation of Epstein-Barr virus from latency following surface immunoglobulin cross-linking. *Proc. Natl. Acad. Sci. USA* 91:772-776.
- Miller, C. L., A. L. Burkhardt, J. H. Lee, B. Stealey, R. Longnecker, J. B. Bolen, and E. Kieff. 1995. Integral membrane protein 2 of Epstein-Barr virus regulates reactivation from latency through dominant-negative effects on protein-tyrosine kinases. *Immunity* 2:155-166.
- Miyashita, E., M., B. Yang, G. J. Babcock, and D. A. Thorley-Lawson. 1997. Identification of the site of Epstein-Barr virus persistence in vivo as a resting B cell. *J. Virol.* 71:4882-4891.
- Nakamura, M., S. E. Burastero, A. L. Norkins, and P. Casali. 1988. Human monoclonal rheumatoid factor-like antibodies from CD5⁺ (Leu-11⁺) B-cell are polyreactive. *J. Immunol.* 140:4180-4186.
- Qu, L., and D. Rowe. 1992. Epstein-Barr virus latent gene expression in uninfected peripheral blood lymphocytes. *J. Virol.* 66:3715-3724.
- Radoux, V., P. P. Chen, J. A. Sorge, and D. A. Carson. 1986. A conserved human germline λ gene directly encodes rheumatoid factor light chains. *J. Exp. Med.* 164:2119-2124.
- Robbins, D. L., W. F. Benisek, E. Benjamin, and R. Wister. 1987. Differential reactivity of rheumatoid synovial cells and serum rheumatoid factors to human immunoglobulin G subclasses 1 and 3 and their CH3 domains in rheumatoid arthritis. *Arthritis Rheum.* 30:489-497.
- Sculley, T. B., P. J. Walker, D. J. Moss, and J. H. Pope. 1984. Identification of multiple Epstein-Barr virus-induced nuclear antigens with sera from patients with rheumatoid arthritis. *J. Virol.* 52:88-93.
- Shimizu, N., H. Yoshiyama, and K. Takada. 1996. Clonal propagation of Epstein-Barr virus (EBV) recombinants in EBV-negative Akata cells. *J. Virol.* 70:7260-7263.
- Takada, K. 1984. Cross-linking of cell surface immunoglobulins induces Epstein-Barr virus in Burkitt lymphoma lines. *Int. J. Cancer* 33:27-32.
- Takada, K., and Y. Ono. 1989. Synchronous and sequential activation of latently infected Epstein-Barr virus genomes. *J. Virol.* 63:445-449.
- Takada, T., Y. Mizogaki, L. Matsubara, S. Inai, T. Koike, and K. Takada. 2000. Lytic Epstein-Barr virus infection in the synovial tissue of patients with rheumatoid arthritis. *Arthritis Rheum.* 43:1218-1225.
- Tierney, R. J., N. Steven, L. S. Young, and A. B. Rickinson. 1994. Epstein-Barr virus latency in blood mononuclear cells: analysis of viral gene transcription during primary infection and in the carrier state. *J. Virol.* 68:7374-7385.
- Tosato, G., A. D. Steinberg, R. Yarehoan, C. A. Heilman, S. E. Pike, V. De Sano, and R. M. Blaese. 1984. Abnormally elevated frequency of Epstein-Barr virus-infected B cells in the blood of patients with rheumatoid arthritis. *J. Clin. Investig.* 73:1789-1795.
- Tovey, M. G., G. Lenoir, and J. Begon-Lours. 1978. Activation of latent Epstein-Barr virus by antibody to human IgM. *Nature* 276:270-272.
- Vaughan, J. H. 1993. Pathogenetic concepts and origins of rheumatoid factor in rheumatoid arthritis. *Arthritis Rheum.* 36:1-6.
- Weiss, A., and D. R. Littman. 1994. Signal transduction by lymphocyte antigen receptors. *Cell* 76:263-274.
- Williams, D. G., S. P. Moyes, and R. A. Mageed. 1999. Rheumatoid factor isotype switch and somatic mutation variants within rheumatoid arthritis synovium. *Immunology* 98:123-136.
- Zimber-Strohl, U., E. Kremmer, F. Grasser, G. Marchall, G. Lawe, and G. W. Borukamm. 1993. The Epstein-Barr virus nuclear antigen 2 interacts with an EBNA2 responsive *cis* element of the terminal protein 1 gene promoter. *EMBO J.* 12:167-175.
- zur Hausen, H., F. J. O'Neill, U. K. Freese, and E. Hecker. 1978. Persisting oncogenic herpesvirus induced by the tumor promoter TPA. *Nature* 272:573-575.
- Zvaifler, N. J. 1973. The immunopathology of joint inflammation in rheumatoid arthritis. *Adv. Immunol.* 16:265-336.



Editorial

Lupus mortality in Japan

Abstract

Systemic lupus erythematosus (SLE)-related mortality has significantly declined in Japan during the past four decades. Decrease in number of deaths due to renal failure has considerably improved the prognosis of SLE. The adequate use of steroid therapy, the new advances in the second-line therapies including immunosuppressants, plasmapheresis and hemodialysis, and the appropriate control of infectious complications are the major reasons of the reduction of SLE-related mortality. The establishment of a nation-wide registration system of SLE in Japan will allow us to improve our strategy to control the disease.

© 2004 Elsevier B.V. All rights reserved.

Keywords: SLE; Mortality; Survival; Japan; Steroids; Immunosuppressants; Renal failure; Cohort; Registration system

Systemic lupus erythematosus (SLE) affects many different organ systems and displays a broad spectrum of clinical and immunologic manifestations. SLE had been recognized as a fatal disease in the beginning of the last century. However in recent years, the prognosis of lupus has been dramatically improved [1–3]. The American College of Rheumatology (ACR) criteria for SLE classification have provided earlier and accurate diagnosis of lupus. It is widely accepted that the establishment of adequate steroid therapy has made a clear difference in the control of SLE. Recent advance in treatment of SLE complications with immunosuppressants has contributed to ameliorate the quality of life and decrease the mortality in lupus nephritis and neuropsychiatric lupus. Appropriate use of plasmapheresis, hemodialysis, and infection control with new antibiotics may contribute to the decrease in mortality of SLE as well. However in a recent study, Cervera et al. [1] showed that 22% of lupus patients died due to active SLE despite the treatment with current therapies.

Ofuji et al. [4] reported the first epidemiological study on SLE in Japan in 1975. One hundred and thirty-nine deaths (11.8%) were observed in 1-year

follow-up of 1185 patients with SLE. The major causes of death were renal failure (36.9%), heart failure (33.3%), infections (15.5%), cerebrovascular disorders (10.7%), suicide (4.9%) and others (9.7%).

Ten years later, Ichikawa et al. [5] in a multicenter study of causes of death in SLE reported that among 212 deaths 74 (34.9%) were due to infections, 41 (19.3%) to cerebrovascular diseases, 19 (9%) to renal failure, 17 (8%) to heart failure and 12 (5.7%) to suicide.

In 1993, Hashimoto et al. [6] reported that the mortality of SLE in Japan has significantly declined during the past four decades. The five-year survival rate of the patients diagnosed from 1955 to 1969 was 71.8%, 1970 to 1979 was 91.3%, and 1980 to 1990 was 96.0%, respectively.

Hashimoto [2] subsequently reported 12 deaths (4%) in 327 cases in his cohort diagnosed from 1986 to 1998, and showed that death due to renal failure dramatically decreased, whereas fatal infections (33%) and pulmonary hypertension (17%) relatively increased as causes of death. These analyses demonstrate that the survival of lupus patients in Japan has greatly improved in the last years. However, failure to

control the disease activity and severe infections still remain as a risk for lupus mortality.

Registration system of SLE started in Japan promoted by the Ministry of Health, Labor, and Welfare. A total of 52,452 patients have been registered by 2002. This is a considerably large cohort to analyze the current characteristics of manifestation, the effectiveness of the therapies, and the accurate prognosis of Japanese patients with SLE. Moreover, this cohort may enable us to compare the safety and efficacy between current therapies and newly developed drugs and to establish a more effective regime for prolonged survival of SLE based on the results.

References

- [1] Cervera R, Khamashta MA, Font J, Sebastiani GD, Gil A, Lavilla P, et al. Morbidity and mortality in systemic lupus erythematosus during a 10-year period: a comparison of early and late manifestations in a cohort of 1,000 patients. *Medicine (Baltimore)* 2003;82(5):299–308.
- [2] Hashimoto H. Changes in the clinical features and prognosis of collagen diseases and their contributing factors: 30 years of past progress and prospect for the 21st century in our department. *Ryumachi* 2001;41(3):672–86.
- [3] Uramoto KM, Michet Jr CJ, Thumboo J, Sunku J, O'Fallon WM, Gabriel SE. Trends in the incidence and mortality of systemic lupus erythematosus, 1950–1992. *Arthritis Rheum* 1999;42(1):46–50.
- [4] Ofuji S, Miyawaki S, Ichikawa Y, Tsunematsu T, Yokohari R, Tanimoto K, et al. Epidemiological studies of systemic lupus erythematosus in Japan. *Ryumachi* 1975;15(3):310–25.
- [5] Ichikawa Y, Tsunematsu T, Yokohari R, Tanimoto K, Sakane T, Yoshida H, et al. Multicenter study of causes of death in systemic lupus erythematosus—a report from the subcommittee for development of therapy, the research committee for autoimmune diseases supported by the ministry of health and welfare. *Ryumachi* 1985;25(4):258–64.
- [6] Hashimoto H, Sugawara M, Tokano Y, Sakamoto M, Isobe Y, Takasaki Y, et al. Follow up study on the changes in the clinical features and prognosis of Japanese patients with systemic lupus erythematosus during the past 3 to 4 decades. *J Epidemiol* 1993;3(1):19–27.

Hiroshi Kataoka*

Takao Koike

*Department of Medicine II, Hokkaido University
Graduate School of Medicine, N-15 W-7, Kita-ku,*

Sapporo 060-8638, Japan

E-mail address: douglas@med.hokudai.ac.jp.

*Corresponding author. Tel.: +81 11 716 1161x5915;
fax: +81 11 706 7710.



A preliminary analysis of the balance between Th1 and Th2 cells after CD34⁺ cell-selected autologous PBSC transplantation

T Endo¹, N Sato², K Koizumi¹, M Nishio¹, K Fujimoto¹, S Yamamoto¹, T Sakai¹, T Bohgaki¹, K Sawada³ and T Koike¹

¹Department of Internal Medicine II, Hokkaido University Graduate School of Medicine, Sapporo, Japan, ²Blood Transfusion Service, Hokkaido University Medical Hospital, Sapporo, Japan, and ³Third Department of Internal Medicine, Akita University School of Medicine, Akita, Japan

Background

CD34⁺ cell-selected autologous PBSC transplantation (CD34⁺ APBSCT) is a procedure used for the treatment of patients with malignant disease that is intended to eliminate residual tumor cells from autologous grafts. However, frequent infectious complications after CD34⁺ APBSCT can occur. A delay of recovery of the absolute number of CD4⁺ T cells after transplantation was reported to be one disadvantageous factor. As data on T-cell function after CD34⁺ APBSCT are scanty, we analyzed changes in T-helper cell 1 (Th1) and T-helper cell 2 (Th2) after CD34⁺ APBSCT to evaluate immune reconstitution.

Methods

Twelve patients underwent APBSCT (CD34⁺ APBSCT group, n = 4, and unselected APBSCT, n = 8). Peripheral blood (PB) samples were obtained at 2, 4, 8, 12 and 16 weeks after the transplantation. The dynamics of the Th1 and Th2 were analyzed at a single-cell level, using flow cytometry.

Results

In the CD34⁺ APBSCT group, not only the absolute count of CD4⁺ T cells but also the proportion of Th1 cells in CD4⁺ T cells and the ratio of Th1 to Th2 after transplantation were significantly decreased at 2 and 4 weeks after transplantation compared with findings in the unselected APBSCT group.

Discussion

We suggest that higher rates of infectious complications after CD34⁺ APBSCT may be due to the inability of residual T cells from the CD34⁺ cell selection to generate mature T cells that function adequately against infection. Although further study would be required, our preliminary data provide some information on the immune reconstitution after CD34⁺ APBSCT and differentiation of T lymphocytes into Th1 and Th2 in vivo.

Keywords

autologous PBSC transplantation, CD34, positive selection, Th1, Th2.

Introduction

High dose chemotherapy followed by autologous PBSC transplantation (APBSCT) is a widely used treatment for patients with malignant disease. The transplantation of selected CD34⁺ cells from PBSC has been used to eliminate residual tumor cells from autologous grafts [1–3]. Studies have shown that CD34⁺ cell-selected APBSCT (CD34⁺ APBSCT) results in a 1–4 log reduction of tumor cells in apheresis products along with prompt hematopoietic reconstitution after myeloablative chemotherapy [1–3]. However, a higher rate of infectious

complications, compared with conventional unselected APBSCT, has been noted [4,5]. A delay of recovery in the absolute number of CD4⁺ T cells after transplantation was reported to be one disadvantageous factor related to CD34⁺ APBSCT [6–8]. There is little documentation on T-cell functions after CD34⁺ APBSCT [9,10].

CD4⁺ T-helper (Th) cells can be divided into two functional subsets, Th1 and Th2 [11]. These cells play important immunoregulatory roles in that Th1 cells secrete IL-2, IFN- γ and tumor necrosis factor (TNF)- β and are involved in cell-mediated immune responses,

Correspondence to: Dr Tomoyuki Endo, Department of Internal Medicine II, Hokkaido University Graduate School of Medicine, N-15, W-7, Kita-ku, Sapporo, Hokkaido 060-8638, Japan.

© 2004 ISCT

DOI: 10.1080/14653240410004907

while Th2 cells produce IL-4, IL-5, IL-6, IL-10 and play a role in humoral responses. Any disorder in the balance of Th1/Th2 subsets may contribute to an impaired T-cell mediated response in clinical states such as infection, cancer and autoimmunity [11]. Although a few reports are available on the Th1/Th2 balance after conventional unselected APBSCT [12], or during acute GvHD after allogeneic blood stem cell transplantation, we found no data on CD34⁺ APBSCT [13,14]. Th1 and Th2 subsets at a single-cell level can be examined readily by measuring intracellular cytokines using flow cytometry [15]. In the present study, we compared the dynamics of the Th1/Th2 balance at a single-cell level after transplantation between CD34⁺ APBSCT and conventional unselected APBSCT, the objective being to assess the immune reconstitution after CD34⁺ APBSCT.

Methods

Patients

Between February 2001 and December 2001, 12 patients aged 19–64 years (median 51 years) underwent a myeloablative conditioning regimen followed by APBSCT at Hokkaido University Hospital (Sapporo, Japan). Individual characteristics of these 12 patients are listed in Table 1. According to the specific protocol active at the time of patient enrollment, two patients with NHL with BM invasion and two patients with systemic sclerosis (SSc) received CD34⁺ APBSCT. The remaining eight patients, six with NHL and two with multiple myeloma (MM), received conventional unselected APBSCT. All patients

gave written informed consent prior to start of the treatment.

Mobilization, collection and cryopreservation of PBSC

For CD34⁺ selection, PBSC were mobilized using the cyclophosphamide, doxorubicin, vincristine, prednisolone (CHOP) regimen [16] ($n=2$) or high-dose CY [17] ($n=2$), each followed by recombinant G-CSF. For patients receiving unselected grafts, PBSC were mobilized with the CHOP ($n=4$) or etoposide, ifosfamide, cisplatin, dexamethasone (VIP) regimen [18] ($n=1$) or high-dose CY ($n=3$), each followed by G-CSF. PBSC collections were made using either Cobe Spectra (Lakewood, CO) or CS3000 (Baxter-Fenwal Division, Deerfield, IL). Unselected PBSC products were cryopreserved with DMSO, as described elsewhere [19].

Selection of CD34⁺ cells

Positive selection of CD34⁺ cells from apheresis products was done using either the Isolex Magnetic Cell Separation System (Isolex 50; Baxter Healthcare, Immunotherapy Division, Newbury, UK) [20,21] or the CliniMACS System (AmCell Corporation, Sunnyvale, CA). Both systems were used according to the manufacturer's specifications.

Transplantation procedure

Pre-transplant conditioning regimens for patients with NHL consisted of ranimustine (MCNU), carboplatin (CBDCA), etoposide (VP-16) and CY (MCVC regimen)

Table 1. Patient data

| # | Age/sex | Diagnosis | Conditioning regimen | Transplantation |
|----|---------|-----------|----------------------|------------------------------------|
| 1 | 54/M | MM | L-PAM | Unselected APBSCT |
| 2 | 48/F | MM | L-PAM | Unselected APBSCT |
| 3 | 38/F | NHL | MCVC | Unselected APBSCT |
| 4 | 31/M | NHL | MCVC | Unselected APBSCT |
| 5 | 61/M | NHL | MCVC | Unselected APBSCT |
| 6 | 59/M | NHL | MCVC | Unselected APBSCT |
| 7 | 64/M | HHL | MCVC | Unselected APBSCT |
| 8 | 54/F | NHL | MCVC | Unselected APBSCT |
| 9 | 19/F | SSc | HD-CY | CD34 ⁺ -selected APBSCT |
| 10 | 53/F | SSc | HD-CY | CD34 ⁺ -selected APBSCT |
| 11 | 41/M | NHL | MCVC | CD34 ⁺ -selected APBSCT |
| 12 | 49/M | NHL | Ara-C/CY/TBI | CD34 ⁺ -selected APBSCT |

[22]. For one patient with NHL, the regimen was cytosine arabinoside (Ara-C), CY and total body irradiation. The regimen for patients with MM was high-dose melphalan (L-PAM). For patients with SSc, the regimen was high-dose CY. All patients were given G-CSF (5 µg/kg/day subcutaneously) from day +1 until engraftment.

Peripheral blood collection and cell isolation

Peripheral blood (PB) samples for Th1/Th2 analysis were obtained prior to pre-transplant conditioning chemotherapy and at 2, 4, 8, 12 and 16 weeks after the transplantation. PB samples from five healthy volunteers served as controls. All PB samples were diluted 1:2 in PBS, layered on Ficoll-Hypaque (Pharmacia Fine Chemicals, Piscataway, NJ) and centrifuged at 400 *g* for 25 min. The interface mononuclear cells were collected, washed twice in PBS and resuspended in IMDM containing 0.3% deionized BSA.

Detection of intracellular cytokine

Mononuclear cells obtained from PB were stimulated with a combination of 50 ng/mL phorbol 12-myristate 13-acetate (PMA) and 1 µg/mL ionomycin in the presence of 10 µg/mL Brefeldin A, and the intracellular protein transport inhibitor then incubated at 37°C in a humidified incubator under 5% CO₂ for 4 h. For non-stimulated controls, aliquots of samples were incubated without PMA and ionomycin, then the cells were stained with 10 µL R-phycoerythrin (RPE)-CY5 conjugated CD4-specific

MAB (DAKO Japan, Kyoto, Japan) for 15 min at room temperature and treated with FACS lysing solution (Becton Dickinson Immunocytometry System, San Jose, CA). After 10 min of incubation, the samples were centrifuged and combined with FACS permeabilizing solution (Becton Dickinson Immunocytometry System) for 10 min at room temperature in the dark, then the samples were washed twice in staining medium (PBS containing 3% FCS and 0.05% sodium azide) and incubated with FITC-conjugated IFN-γ-specific MAb and PE-conjugated IL-4-specific MAb (Becton Dickinson Biosciences, San Jose, CA) for 30 min at room temperature in the dark. After washing twice more with staining medium, the samples were analyzed using flow cytometry.

Flow cytometry

Samples were run through a FACS Calibur flow cytometer (Becton Dickinson Biosciences). A minimum of 50 000 events was analyzed, using CellQuest software (Becton Dickinson Biosciences). The three-color flow cytometry technique was used to analyze IFN-γ and IL-4 expression in CD4⁺ T cells [15]. For an accurate CD4⁺ T-cell evaluation, CD4^{dim} events were excluded from analysis to exclude monocytes. CD4⁺/IFN-γ⁺/IL-4⁻ cells and CD4⁺/IFN-γ⁻/IL-4⁺ cells were assumed to be Th1 and Th2 cells, respectively (Figure 1). The percentages of Th1 and Th2 were evaluated by the ratio of CD4⁺/IFN-γ⁺/IL-4⁻ cells and CD4⁺/IFN-γ⁻/IL-4⁺ to total CD4⁺ cells, respectively. The Th1/Th2 balance were

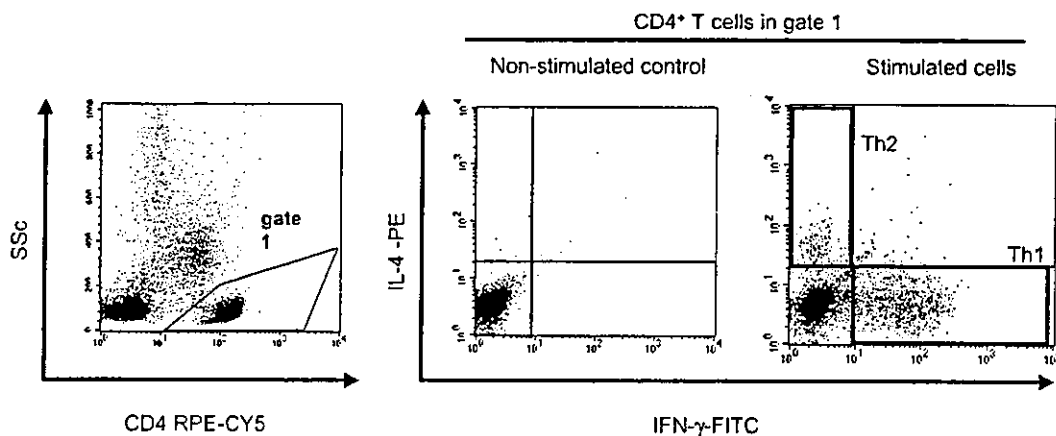


Figure 1. Detection of Th1 and Th2 cells. CD4⁺ T cells were gated by a dot plot analysis, side scatter (vertical axis) vs. right angle RPE-CY5 light scatter (horizontal axis). Non-stimulated cells served as negative controls. The percentages of IFN-γ⁺/IL-4⁻ cells (lower right column) and IFN-γ⁻/IL-4⁺ cells (upper left column) in the CD4⁺ gated cells were assumed to be Th1 and Th2 cells. The Th1/Th2 balance was evaluated by the ratio of CD4⁺/IFN-γ⁺/IL-4⁻ cells to CD4⁺/IFN-γ⁻/IL-4⁺ cells.

evaluated based on the ratio of CD4⁺/IFN- γ ⁺/IL-4⁻ cells to CD4⁺/IFN- γ ⁻/IL-4⁺ cells.

Statistical methods

Comparisons between the group of patients given CD34⁺ APBSCT and those undergoing conventional unselected APBSCT were made using the Mann-Whitney *U*-test. Values of *P* < 0.05 were considered significant.

Results

Transplanted cells

Numbers of transplanted CD34⁺ and colony-forming units-granulocyte/macrophage (CFU-GM) cells are shown in Table 2. These numbers were sufficient to transplant both CD34⁺ APBSCT and unselected APBSCT groups. Highly purified CD34⁺ cells (90.2–98.1%) were obtained using positive selection procedures.

Engraftment

For all patients neutrophil engraftment was achieved after a median of 9.5 (range 8–12) days (Table 2). No significant difference was found between each group. In the CD34⁺ APBSCT group, the absolute number of peripheral CD4⁺ T cells at 4 weeks after stem cell infusion was significantly decreased compared with the findings in the unselected APBSCT group (*P* < 0.05) (Table 2).

Infectious complications

In the CD34⁺ APBSCT group, infectious complications after transplantation occurred in three patients (75%); cytomegalovirus pneumonia, pericarditis, and adenovirus hemorrhagic cystitis in one patient, neutropenic fever in another patient, and bacterial pneumonia, pericarditis and pleurisy in the other patient. Infection occurred in two patients (25%) in the unselected APBSCT group; *Aspergillus* pneumonia in one patient, and neutropenic fever in the other patient (Table 2).

Th1 and Th2 cells after APBSCT

Changes in Th1 and Th2 cells after APBSCT are shown in Figure 2. In CD34⁺ APBSCT, the proportion of Th1 cells among CD4⁺ T cells was significantly decreased at 2 and 4 weeks after transplantation compared with findings in unselected APBSCT. On the other hand, the proportion of Th2 cells in CD4⁺ T-cells showed no difference. The ratio of Th1 to Th2 in CD34⁺ APBSCT was significantly decreased at 2 and 4 weeks after transplantation compared with cases of unselected APBSCT. The proportion of Th1 cells and the ratio of Th1 to Th2 after 8 weeks in both groups were increased compared with findings in normal controls.

Discussion

In this study, we found that the Th1/Th2 balance after CD34⁺ APBSCT differs from unselected APBSCT, that

Table 2. Transplanted cells, engraftment and infectious complications.

| # | CD34 ⁺ cells | | CFU-GM No. ($\times 10^5$ /kg) | Neutrophil > 0.5×10^9 /L (day) | CD4 ⁺ T-cell number at 4 weeks after PBSCT ($\times 10^6$ /L) | Infection-related complications |
|----|--------------------------|-------------------|------------------------------------|---|---|--|
| | No. ($\times 10^6$ /kg) | Purity (% MNC) | | | | |
| 1 | 2.51 | 0.57 | 1.97 | 10 | 90.83 | <i>Aspergillus</i> pneumonia |
| 2 | 2.84 | 1.39 | 5.70 | 9 | 353.57 | Neutropenic fever |
| 3 | 3.34 | 1.48 | 8.74 | 8 | 285.12 | (-) |
| 4 | 2.36 | 1.26 | 1.98 | 9 | 187.62 | (-) |
| 5 | 2.79 | 3.15 | 4.39 | 10 | 135.25 | (-) |
| 6 | 2.48 | 0.69 | 6.47 | 10 | 196.77 | (-) |
| 7 | 1.64 | 0.20 | 1.94 | 10 | 424.51 | (-) |
| 8 | 3.00 | 1.21 | 5.66 | 9 | 323.57 | (-) |
| 9 | 5.21 | 96.0 | 27.80 | 9 | 17.66 | (-) |
| 10 | 2.75 | 90.2 | 4.47 | 12 | 1.37 | CMV pneumonia, pericarditis, adenovirus cystitis |
| 11 | 10.90 | 98.1 | 15.17 | 10 | 191.16 | Neutropenic fever |
| 12 | 4.03 | 96.0 | 13.30 | 9 | 72.55 | Bacterial pneumonia, pericarditis, pleurisy |

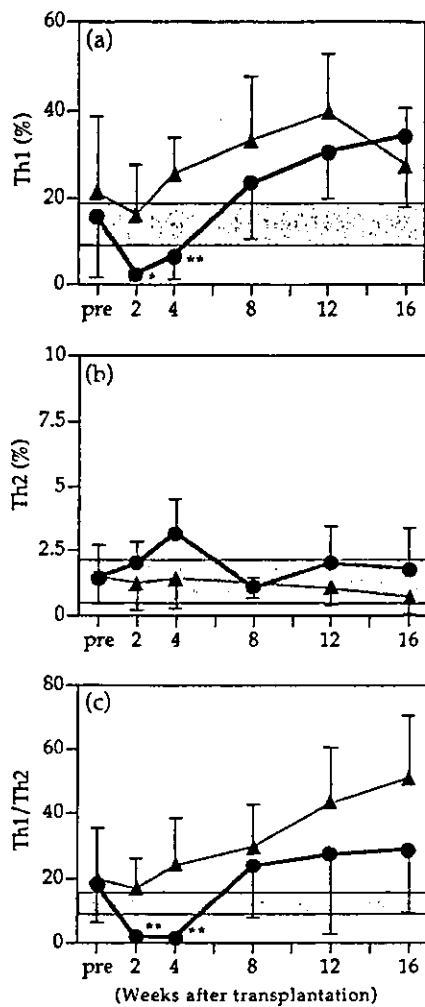


Figure 2. Changes of Th1 and Th2 cells after unselected APBSCT (▲) and CD34⁺-selected APBSCT (●). Data are the mean and standard deviations. The shaded areas are the standard deviations in healthy volunteers who served as normal controls. (a) In CD34⁺-selected APBSCT, the proportion of Th1 cells in CD4⁺ T cells was significantly decreased at 2 and 4 weeks after transplantation compared with the value of unselected APBSCT. (b) Proportion of Th2 cells in CD4⁺ T cells showed no differences. (c) The ratio of Th1 to Th2 in CD34⁺-selected APBSCT was significantly decreased at 2 and 4 weeks after transplantation compared with the value of unselected APBSCT. *P < 0.05 decrease compared with the value of unselected APBSCT. **P < 0.01 decrease compared with the value of unselected APBSCT.

is, not only the absolute count of CD4⁺ T cells but also the proportion of Th1 cells in CD4⁺ T cells and the ratio of Th1 to Th2 were significantly decreased in the CD34⁺-selected APBSCT group.

Th1 cells play an important role in cell-mediated immune responses. The balance is also important, because

Th1 and Th2 are equipped with mechanisms to down-regulate each other. The disorder of Th1/Th2 balance may contribute to impaired T-cell mediated response in clinical states such as infection [11]. Essa *et al.* [23] reported that the levels of Th1-type cytokines in kidney transplant recipients were significantly lower in CMV-infected patients than in uninfected patients, yet the Th2-type cytokine in both cases was similar. They suggested that the low level of Th1-type cytokines correlated with active CMV infection. Sparrelid *et al.* [24] reported similar observations in the setting of allogeneic BMT; recipients with interstitial pneumonitis had a low level of Th1 cytokine production whereas Th2 cytokine production remained unaltered. The study of Essa *et al.* [23] and that of Sparrelid *et al.* [24] dealt with the Th1/Th2 balance at a serum cytokine level and on local production of cytokines levels within the lung, respectively. On the other hand, our present study dealt with the Th1/Th2 balance at a single-cell level, determined by measurement of intracellular cytokines. The results of the present study suggest that higher rates of infectious complications after CD34⁺ APBSCT may be due to the inability of residual T cells to generate mature Th1 cells with sufficient functions to counterattack infection. In fact, most infectious complications after CD34⁺ APBSCT occur 2–4 weeks after transplantation, a time period that coincides with the time that Th1 cells and the ratio of Th1 to Th2 are decreased.

Studies of the Th1/Th2 balance after CD34⁺ APBSCT are important to observe the maturation of helper T lymphocytes. In our study, patients treated with CD34⁺ APBSCT were given highly purified CD34⁺ cells after myeloablative therapy, so the influence from other blood cells except for transplanted CD34⁺ cells was thought to be minimum. Our data seem to be the first assessment of changes in the Th1/Th2 balance at a single-cell level after CD34⁺ APBSCT and may be useful as a model of the differentiation of Th1 and Th2 from hematopoietic stem cells *in vivo*.

It is not clear why the Th1/Th2 balance shows Th2 dominance after CD34⁺ APBSCT. One possibility is differences in the original disease between the groups. However, the Th1/Th2 balance in both groups was similar in the pre-transplantation period, so there is little possibility that the original disease is related to the difference in Th1/Th2 balance after transplantation. Th1 and Th2 cells develop from a common pool of naive Th

cells [11]. Although the commitment toward either the Th1 or the Th2 can be influenced by many factors, the levels of IL-12 and IL-4 are of major importance [25,26]. Development of Th1 and Th2 cells displays a substantial requirement for IL-12 and IL-4, respectively, as demonstrated using gene-knockout mice [26–28]. IL-12 is produced primarily by monocytes, macrophages, DC) and B cells. This leads naive Th cells to Th1 cells and inhibits the generation of Th2. On the other hand, it has been reported that naive Th cells could secrete IL-4 and drive their own development towards a Th2 phenotype [29]. In this study, we did not measure serum cytokine levels or the local production of cytokines, such as in BM. However, the decrease in the proportion of Th1 cells after CD34⁺ APBSCT may result from an absence of IL-12 producing cells, such as macrophage and DC, after transplantation of highly purified CD34⁺ cells following myeloablative therapy, while the commitment move toward Th2 cells may be maintained by IL-4 secreted from the naive Th cell itself.

Further study on a larger group of patients with homogeneous disease is required to validate these findings, but our preliminary data provide some information on the immune reconstitution after CD34⁺ APBSCT and differentiation of T lymphocytes into Th1 and Th2 *in vivo*.

Acknowledgements

We thank M. Kitayama and I. Sato for technical assistance.

References

- Schiller G, Vescio R, Freytes C *et al.* Transplantation of CD34⁺ peripheral blood progenitor cells after high-dose chemotherapy for patients with advanced multiple myeloma. *Blood* 1995;86:390–7.
- McQuaker IG, Haynes AP, Anderson S *et al.* Engraftment and molecular monitoring of CD34⁺ peripheral-blood stem-cell transplants for follicular lymphoma: a pilot study. *J Clin Oncol* 1997;15:2288–95.
- Abonour R, Scott KM, Kunkel LA *et al.* Autologous transplantation of mobilized peripheral blood CD34⁺ cells selected by immunomagnetic procedures in patients with multiple myeloma. *Bone Marrow Transplant* 1998;22:957–63.
- Holmberg LA, Boeckh M, Hooper H *et al.* Increased incidence of cytomegalovirus disease after autologous CD34-selected peripheral blood stem cell transplantation. *Blood* 1999;94:4029–35.
- Friedman J, Lazarus HM, Koc ON. Autologous CD34⁺ enriched peripheral blood progenitor cell (PBPC) transplantation is associated with higher morbidity in patients with lymphoma when compared to unmanipulated PBPC transplantation. *Bone Marrow Transplant* 2000;26:831–6.
- Takeshima M, Takamatsu H, Iida M *et al.* Frequent viral infections and delayed CD4⁺ cell recovery following CD34⁺ cell-selected autologous peripheral blood stem cell transplantation. *Int J Hematol* 1999;70:193–9.
- Rutella S, Rumi C, Laurenti L *et al.* Immune reconstitution after transplantation of autologous peripheral CD34⁺ cells: analysis of predictive factors and comparison with unselected progenitor transplants. *Br J Haematol* 2000;108:105–15.
- Nishio M, Koizumi K, Endo T *et al.* Diminished T-cell recovery after CD34⁺ selected autologous peripheral blood stem cell transplantation increases the risk of cytomegalovirus infection. *Haematologica* 2001;86:667–8.
- Nachbaur D, Kropshofer G, Heitger A *et al.* Phenotypic and functional lymphocyte recovery after CD34⁺-enriched versus non-T cell-depleted autologous peripheral blood stem cell transplantation. *J Hematother Stem Cell Res* 2000;9:727–36.
- Rutella S, Pierelli L, Sica S *et al.* Transplantation of autologous peripheral blood progenitor cells: impact of CD34-cell selection on immunological reconstitution. *Leuk Lymphoma* 2001;42:1207–20.
- Lucey DR, Clerici M, Shearer GM. Type 1 and type 2 cytokine dysregulation in human infectious neoplastic and inflammatory diseases. *Clin Microbiol Rev* 1996;9:532–62.
- Mukai M, Bohgaki T, Kondo M *et al.* Changes in the T-helper cell 1/T-helper cell 2 balance of peripheral T-helper cells after autologous peripheral blood stem cell transplantation for non-Hodgkin's lymphoma. *Ann Hematol* 2001;80:715–21.
- Carayol G, Bourhis JH, Guillard M *et al.* Quantitative analysis of T helper 1, T helper 2, and inflammatory cytokine expression in patients after allogeneic bone marrow transplantation. *Transplantation* 1997;63:1307–13.
- Tanaka J, Imamura M, Kasai M *et al.* The important balance between cytokines derived from type 1 and type 2 helper T cells in the control of graft-versus-host disease. *Bone Marrow Transplant* 1997;19:571–6.
- Openshaw P, Murphy EE, Hosken NA *et al.* Heterogeneity of intracellular cytokine synthesis at single-cell level in polarized T helper 1 and T helper 2 populations. *J Exp Med* 1995;182:1357–67.
- Takano H, Sawada K, Sato N *et al.* Mobilization of peripheral blood progenitor cells following CHOP treatment combined with delayed granulocyte colony-stimulating factor administration in patients with non-Hodgkin's lymphoma. *Leuk Lymphoma* 1996;21:473–8.
- Vesole DH, Tricot G, Jagannath S *et al.* Autotransplants in multiple myeloma: what have we learned? *Blood* 1996;88:838–47.
- Brugger W, Frisch J, Schulz G *et al.* Sequential administration of interleukin-3 and granulocyte-macrophage colony-stimulating factor following standard-dose combination chemotherapy with etoposide, ifosfamide, and cisplatin. *J Clin Oncol* 1992;10:1452–9.

- 19 Koizumi K, Nishio M, Endo T *et al.* Large scale purification of human blood CD34⁺ cells from cryopreserved peripheral blood stem cells, using a nylon-fiber syringe system and immunomagnetic microspheres. *Bone Marrow Transplant* 2000;26:787–93.
- 20 Koizumi K, Sawada K, Sato N *et al.* Large scale purification of human blood CD34⁺ cells using nylon-fiber syringe system and immunomagnetic microspheres. *Cytotherapy* 1999;1:319–27.
- 21 Yamaguchi M, Sawada K, Sato N *et al.* A rapid nylon-fiber syringe system to deplete CD14⁺ cells for positive selection of human blood CD34⁺ cells, Use of immunomagnetic microspheres. *Bone Marrow Transplant* 1997;19:373–9.
- 22 Tarumi T, Sawada K, Koizumi K *et al.* A pilot study of a response oriented chemotherapeutic regimen combined with autologous peripheral blood progenitor cell transplantation in aggressive non-Hodgkin's lymphoma. *Leuk Lymphoma* 1999;34:361–71.
- 23 Essa S, Raghupathy R, Pacsa AS *et al.* Th1-type cytokines production is decreased in kidney transplant recipients with active cytomegalovirus infection. *J Med Virology* 2000;60:223–9.
- 24 Sparrelid E, Emanuel D, Fehniger T *et al.* Interstitial pneumonitis in bone marrow transplant recipients is associated with local production of TH2-type cytokines and lack of T cell-mediated cytotoxicity. *Transplantation* 1997;63:1782–9.
- 25 Vieira PL, de Jong EC, Wierenga EA *et al.* Development of Th1-inducing capacity in myeloid dendritic cells requires environmental instruction. *J Immunol* 2000;164:4507–12.
- 26 Noble A, Thomas MJ, Kemeny DM. Early Th1/Th2 cell polarization in the absence of IL-4 and IL-12: T cell receptor signaling regulates the response to cytokines in CD4 and CD8 T cells. *Eur J Immunol* 2001;31:2227–35.
- 27 Magram J, Connaughton SE, Warriar RR *et al.* IL-12-deficient mice are defective in IFN γ production and type 1 cytokine responses. *Immunity* 1996;4:471–81.
- 28 Kuhn R, Rajewsky K, Muller W. Generation and analysis of interleukin-4 deficient mice. *Science* 1991;254:707–10.
- 29 Ouyang W, Lohning M, Gao Z *et al.* Stat6-independent GATA-3 autoactivation directs IL-4-independent Th2 development and commitment. *Immunity* 2000;12:27–37.

Novel Negative Regulator of Expression in Fas Ligand (CD178) Cytoplasmic Tail: Evidence for Translational Regulation and against Fas Ligand Retention in Secretory Lysosomes¹

Sheng Xiao,* Umesh S. Deshmukh,* Satoshi Jodo,[†] Takao Koike,[†] Rahul Sharma,* Akiro Furusaki,[†] Sun-sang J. Sung,* and Shyr-Te Ju^{2*}

Fas ligand (FasL) CD178, a type II transmembrane protein, induces apoptosis of cells expressing the Fas receptor. It possesses a unique cytoplasmic tail (FasL_{CYT}) of 80 aa. As a type II transmembrane protein, the early synthesis of FasL_{CYT} could affect FasL translation by impacting FasL endoplasmic reticulum translocation and/or endoplasmic reticulum retention. Previous studies suggest that the proline-rich domain (aa 43–70) in FasL_{CYT} (FasL_{PRD}) inhibits FasL membrane expression by retaining FasL in the secretory lysosomes. This report shows that deletion of aa 2–33 of FasL_{CYT} dramatically increased total FasL levels and FasL cell surface expression. This negative regulator of FasL expression is dominant despite the presence of FasL_{PRD}. In addition, retention of proline-rich domain-containing FasL in the cytoplasm was not observed. Moreover, we demonstrated that FasL_{CYT} regulates FasL expression by controlling the rate of de novo synthesis of FasL. Our study demonstrated a novel negative regulator of FasL expression in the FasL_{CYT} region and its mechanism of action. *The Journal of Immunology*, 2004, 173: 5095–5102.

Fas (CD95) is a type I transmembrane protein expressed by many nucleated cells (1–3). The physiological Fas ligand (FasL)³ is a type II transmembrane protein expressed by activated T cells and non-T cells under a variety of conditions (4–6). The extracellular domain of FasL (FasL_{EXT}) on effector cells binds to Fas on target cells and cross-linking of Fas induces target cells to undergo apoptosis (7–9). The Fas/FasL-mediated apoptosis pathway has been implicated in immune response regulation (9, 10), peripheral tolerance (5, 11–15), graft rejection (16–18), tumor surveillance (19), tissue pathology (20–22), chemotaxis (17, 18, 23), and maintenance of the immune privileged sites (24, 25).

Regulation of FasL expression has been demonstrated at the transcriptional and posttranslational levels. At the transcriptional level, the *FasL* gene is regulated by different transcription factors, depending on cell types and experimental conditions (25–33). At the posttranslational level, cell surface FasL can be removed by metalloproteinase cleavage that generates soluble FasL, which is a poor mediator of cytotoxicity (34, 35). Recent studies also showed that FasL are released from cells in the form of vesicles (36–38). In contrast to soluble FasL, these vesicles contain full-length FasL and express potent cytotoxic activity (37).

FasL is a member of the TNF family but it possesses a unique 80-aa cytoplasmic tail (FasL_{CYT}) that is highly conserved among

species (39). As a type II transmembrane protein, FasL_{CYT} may have motifs that can regulate FasL translation and processing soon after its de novo protein synthesis begins. Recent studies suggest that the proline-rich domain (PRD) of FasL_{CYT} regulates FasL cell surface expression by retaining FasL in the secretory lysosomes (40, 41). Moreover, cells lacking secretory lysosomes strongly expressed cell surface FasL upon transfection with the *fasl* gene (41). However, these studies were conducted with constructs whose 5' ends were attached to *GFP* gene. Thus, the effects of GFP, a large protein with ~220 aa, on FasL_{CYT} functions in FasL translation, translocation, processing, and trafficking cannot be ruled out. In addition, the use of GFP-based fluorescence microscopy and flow cytometry makes an accurate quantitative analysis of total FasL expression by transfected cells difficult.

To better define the role of FasL_{CYT} in the translational regulation of FasL expression, we engineered various deletion constructs of human *fasl* gene without a GFP tag, used these constructs to generate stable transfectants of various cell lines, conducted quantitative ELISA for FasL, and determined their de novo synthesis rates and their homeostatic expression levels. We found that FasL_{CYT} negatively regulates FasL cell surface expression by limiting its total cellular expression level. The responsible region was located between aa 2–33 (FasL_{2–33}). In addition, we observed that fully expressed FasL containing the PRD was not selectively retained in the cytoplasm. Instead, FasL_{CYT} regulates FasL expression by controlling the rate of FasL de novo synthesis. Our study demonstrates the presence of a novel negative regulator of FasL expression in the FasL_{CYT} region and identifies its mechanism of action.

Materials and Methods

Cell lines and reagents

Neuro-2a (mouse neuroblastoma), NIH-3T3 (mouse fibroblast), B16F1 (mouse melanoma), rat basophilic leukemia (RBL), and COS-7 (monkey kidney fibroblast) cell lines were obtained from American Type Culture Collection (Manassas, VA). Culture medium was prepared by supplementing high glucose (4.5 g/L) DMEM (Cellgro; Mediatech, Herndon, VA) with 10% heat-inactivated FCS (Invitrogen Life Technologies, Carlsbad,

*Department of Internal Medicine, Division of Rheumatology and Immunology, University of Virginia, Charlottesville, VA 22908; and [†]Department of Medicine II, Hokkaido University Graduate School of Medicine, Kita-ku, Sapporo, Japan

Received for publication May 18, 2004. Accepted for publication August 9, 2004.

The costs of publication of this article were defrayed in part by the payment of page charges. This article must therefore be hereby marked *advertisement* in accordance with 18 U.S.C. Section 1734 solely to indicate this fact.

¹ This work was supported in part by National Institutes of Health Grant AI36938 (to S.-T.J.) and HL07065 (to S.-S.J.S.), and a grant from the American Heart Association (to U.S.D.).

² Address correspondence and reprint requests to Dr. Shyr-Te Ju, Department of Internal Medicine, Division of Rheumatology and Immunology, University of Virginia, Charlottesville, VA 22908-0412. E-mail address: sjr@virginia.edu

³ Abbreviations used in this paper: FasL, Fas ligand; PRD, proline-rich domain; snRNP, small nuclear ribonucleoproteins; Vc, vector control; WT, wild type; RBL, rat basophilic leukemia; ER, endoplasmic reticulum; CKI, casein kinase I.

CA), 100 U/ml penicillin, 100 µg/ml streptomycin, 1 mM l-glutamine, 1 mM sodium pyruvate, and 5 µg/L of 2-ME. PE-A1F-2.1 anti-human FasL mAb was purchased from Caltag Laboratories (Burlingame, CA). PE-NOK-1 and FITC-NOK-1 anti-human FasL mAb were purchased from Santa Cruz Biotechnology (Santa Cruz, CA). Unlabeled G247.4 and NOK-1 anti-FasL mAb were obtained from BD Biosciences (San Diego, CA). All restriction endonucleases were obtained from New England Biolabs (Beverly, MA). The prokaryotic expression vector pBlueScript II KS was obtained from Stratagene (La Jolla, CA). The human *FasL* cDNA construct and the mammalian expression vector BCMGSneo (14.5 kb) were kindly provided by Dr. S. Nagata (Osaka University Medical Center, Osaka, Japan) (39).

Construction of FasL deletion mutants

The full-length *hfasl* cDNA cloned in the pBlueScript II KS was used to generate deletion mutants by PCR using different 5' primers and the same 3' primer. All 5' primers used contain the translation start sequence ATG (shown in bold) that codes for methionine. Because methionine is the first amino acid of wild-type (WT) and deletion mutants, deletion begins with amino acid residue 2 of FasL. All primers were obtained from Integrated DNA Technologies (Coralville, IA). The sequences of the 5' primers are 5'-ATGACCTCTGTGCCAGAAGGCC-3' (for Δ33 in which FasL₂₋₃₃ is deleted), 5'-ATGCTGAAGAAGAGAGGGGAACACAGC-3' (for Δ70 in which FasL₂₋₇₀ is deleted), and 5'-ATGCAGCTCTCCACCTACA GAAGGAGC-3' (for Δ102 in which FasL₂₋₁₀₂ is deleted). The sequence of the 3' primer is 5'-GTAAAACGACGGCCAGTGAAGC-3'. The PCR products were subcloned into pBlueScript II KS. These inserts were excised with *NorI* and *XhoI* and cloned into BCMGSneo vector (39). Gene sequences of each construct were confirmed by DNA sequencing.

Transfection

Multiple cell lines were transfected with the expression constructs using PolyFect Transfection Reagent (Qiagen, Valencia, CA) according to the manufacturer's protocol. Briefly, cells (8×10^5 per 60-mm dish) were seeded in 5 ml of culture medium the day before transfection. Culture medium was replaced with 3 ml of DMEM before transfection. To prepare transfection mixtures, 2.5 µg of plasmid DNA were diluted with DMEM to 150 µl, and 15 µl of PolyFect transfection reagent was added. After incubation for 10 min at room temperature, the transfection mixtures were mixed with 1 ml of DMEM and immediately transferred to dishes containing seeded cells. Dishes were gently swirled, cultured for 24 h, and then replaced with culture medium containing 0.4 mg/ml G418 (Invitrogen Life Technologies). Cell populations that survived the G418 selection were expanded in G418-containing culture medium and examined. Typically, the selection process takes 3–4 wk to complete. Expanded cells were analyzed and aliquots were stored in liquid nitrogen tank.

Flow cytometric analysis

To determine cell surface expression of FasL, cells (0.3×10^6) were suspended in 100 µl of PBS containing 4% BSA and incubated with 1 µg of PE-A1F-2.1 mAb or PE-conjugated isotype control for 45 min at 4°C. Reaction mixtures were gently mixed periodically. Cells were washed twice with cold PBS and then analyzed. To determine both cell surface and intracellular expression of FasL, cells were first stained with 2 µg of FITC-NOK-1 mAb for 45 min at 4°C. After washing, labeled cells were fixed for 20 min at room temperature in 2% paraformaldehyde, permeated with 0.1% saponin, and then stained with PE-NOK-1 mAb. Using the same anti-FasL mAb prevented cell surface staining by PE-NOK-1 mAb. At least 10^4 stained cells were analyzed using FACScan equipped with CellQuest software (BD Biosciences).

Confocal microscopic analysis

Various transfectants were first stained with 2 µg of FITC-NOK-1 mAb at 4°C. After washing, labeled cells were fixed for 20 min in 2% paraformaldehyde, permeated with 0.1% saponin, and then stained with PE-NOK-1 mAb. The stained cells were examined using a Carl Zeiss LSM 510 confocal microscope (Carl Zeiss, Thornwood, NY).

Cell-mediated cytotoxicity

Cell-mediated cytotoxicity was conducted as previously described using the ⁵¹Cr-labeled, Fas⁺ A20 B lymphoma target cells (38). Transfectants were incubated with 2×10^4 target cells at various E:T ratios for 5 h at 37°C in a 10% CO₂ incubator. Cell-free supernatants were collected and counted with a gamma counter (LKB, Turku, Finland). Cytotoxicity, expressed as percent of specific Cr-release, was calculated by the formula: $100 \times (\text{experimental release} - \text{background release}) / (\text{total release} - \text{back-$

ground release). Background release was obtained by culturing target cells with medium and total release was determined by lysing target cells with 2% Triton X-100. Experiments were performed in duplicate and repeated at least twice.

FasL-specific ELISA

Cells (10^7) were treated with Ag-extraction buffer provided with the FasL ELISA kit (Oncogene, Boston, MA). All samples were diluted in sample dilution buffer (provided with the kit) and immediately assayed. Standard curves were generated with various molar concentrations of recombinant soluble FasL. The amount of FasL in each sample was calculated and converted to picomoles based on the molecular weights of the engineered FasL proteins.

FasL mRNA analysis

Total RNA was extracted with TRIzol reagent (Invitrogen Life Technologies). FasL and β-actin mRNA was measured by RT-PCR essentially as previously described (42), but our re-designed primers detected FasL mRNA irrespective of their introduced deletion. The sequences of the forward and reverse primers for FasL were 5'-AACTCCGAGAGTCTAC CAGCCAG-3' and 5'-GATACTTAGAGTTCCTCATGTAGACC-3', respectively. FasL mRNA was also determined by RNase protection assays using the customized RiboQuant Multiprobe Template set (BD Biosciences). This template set was designed to specifically quantitate mouse L32, mouse GAPDH, and human FasL transcripts.

[³⁵S]Methionine labeling of FasL

Various transfectants were [³⁵S]methionine-labeled ([³⁵S]Express; PerkinElmer, Boston, MA) for the indicated times as previously described (43). Cells were subsequently lysed with 0.05 M Tris-HCl buffer (pH 8.0) containing 0.3 M NaCl, protease inhibitor mixture (Sigma-Aldrich, St. Louis, MO), 2 mM EDTA, and 0.5% Nonidet P-40. NOK-1 mAb (10 µg) was adsorbed onto Protein A/G Plus-agarose (20 µl) (Amersham Biosciences, Piscataway, NJ) for 1 h at room temperature, followed by incubation with cell lysates for 2 h at 4°C. As an internal control, aliquots of lysates were also incubated with a mouse polyclonal anti-small nuclear ribonucleoproteins (snRNP) Abs adsorbed onto Protein A/G Plus-agarose. After extensive washing, bound proteins were released from beads by boiling in SDS-PAGE loading buffer and analyzed by 12% SDS-PAGE. Gels were dried and autoradiographed.

Results

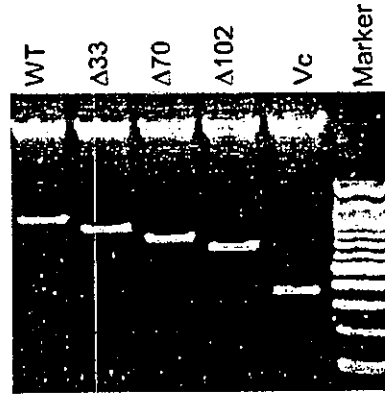
FasL_{C₂₇} regulates FasL cell surface expression

To define the role of FasL_{C₂₇} in regulating FasL expression, we generated various deletion constructs of human *fasl* gene (Fig. 1a). The insert sizes were confirmed in digests using restriction endonucleases *NorI* and *XhoI* (Fig. 1a). Their sequences were confirmed by DNA sequence analyses (see *Materials and Methods*). These expression vectors were transfected into various cell types and G418-resistant cell lines were selected. FasL cell surface expression on the selected cell lines was assessed by flow cytometry using the anti-FasL_{C₂₇} mAb (Fig. 1b). Although WT FasL transfectants displayed a relatively low level of membrane FasL, deletion of aa 2–33 from FasL (Δ33 FasL) resulted in a significant increase in FasL cell surface expression. This trend was observed in all of the cell lines examined. However, there was variability in expression among individual experiments. Deleting aa 2–70 (Δ70 FasL) that contained the PRD further increased the percentage of FasL expression in Neuro-2a, RBL, and B16F1 transfectants (Fig. 1b), but not appreciably in the NIH-3T3 or COS-7 transfectants. In the latter case, the mean fluorescence intensity was slightly increased. Membrane FasL was not detected in vector control (Vc) or Δ102 FasL transfectants. Δ102 FasL was not expressed on cell membrane because it lacked an intact transmembrane domain.

Cell-mediated cytotoxicity of various transfectants

FasL expression on various transfectants was determined with a mAb reactive with FasL_{C₂₇} that is presumably not modified by the deletion. To determine whether FasL transfectants were functional, we conducted cell-mediated cytotoxicity using FasL-sensitive A20

a



b

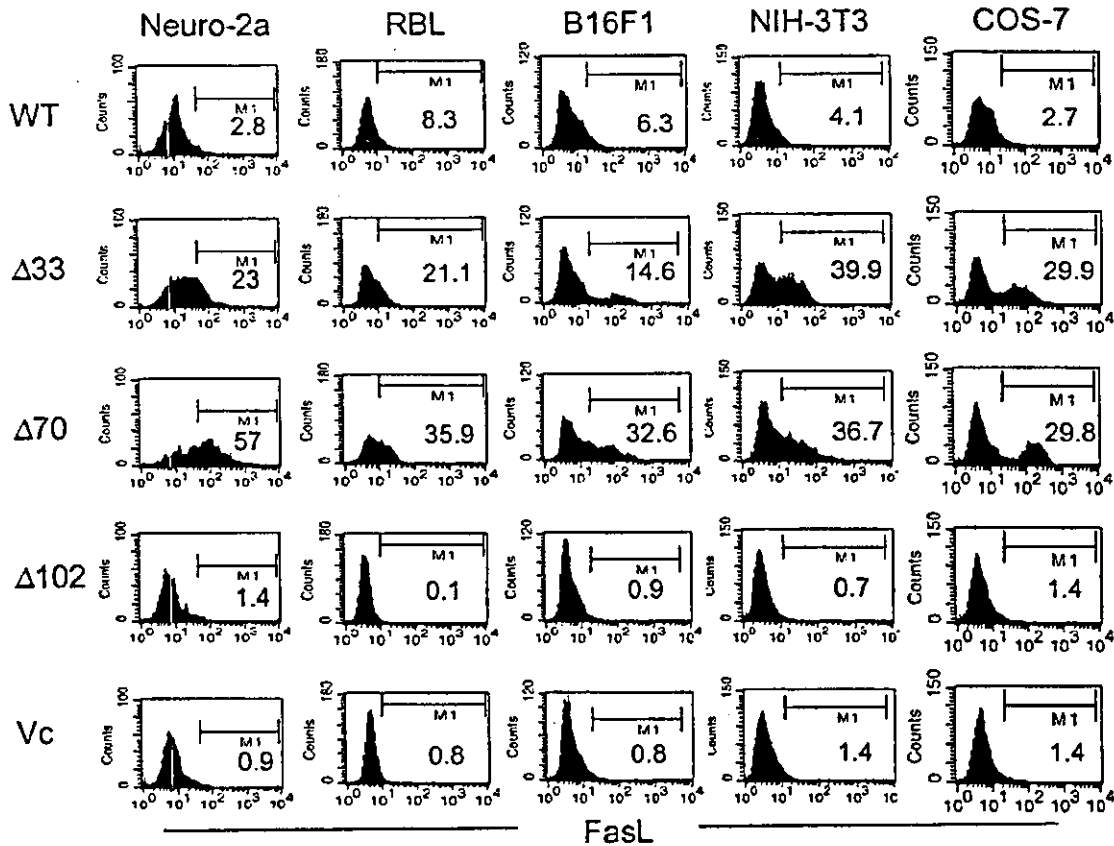
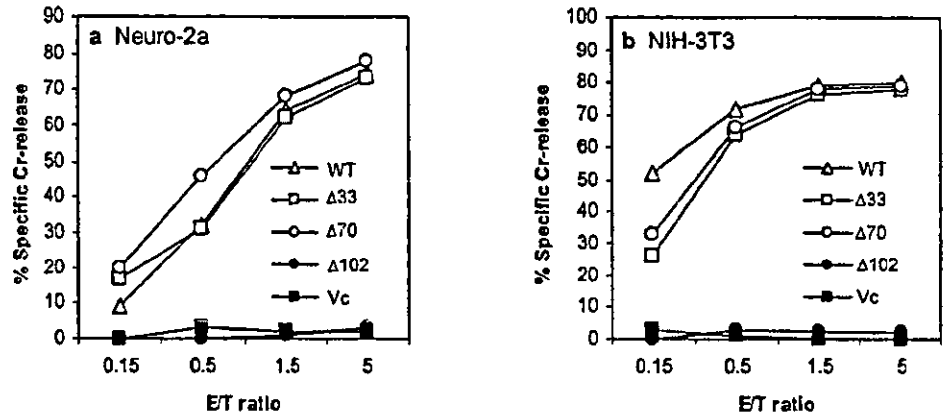


FIGURE 1. Sequence map of various FasL constructs used for transfection and FasL cell surface expression on various transfected cell lines. *a*, Deletion mutants used in this study. Deletion mutants of FasL cytoplasmic tail ($\Delta 33$, $\Delta 70$, and $\Delta 102$) were made as described in *Materials and Methods*. Because methionine residue is the first amino acid of WT and deletion mutants, $\Delta 33$, $\Delta 70$, and $\Delta 102$ represent mutants in which FasL₂₋₃₃, FasL₂₋₇₀ and FasL₂₋₁₀₂ were deleted, respectively. The PRD is underlined. TM indicates transmembrane domain. The insert sizes of FasL deletion constructs were confirmed by excising the inserts from vectors using restriction endonucleases *XhoI* and *NotI*. The digests were analyzed by agarose gel electrophoresis. The sizes of WT, $\Delta 33$, $\Delta 70$, and $\Delta 102$ inserts are ~1000, ~850, ~750, and ~650 bp, respectively. The Vc contains a stuffer of ~350 bp between *XhoI* and *NotI*. *b*, N-terminal deletion of FasL₂₋₃₃ and FasL₂₋₇₀ resulted in an increase in FasL cell surface expression. Expression vectors of WT, $\Delta 33$, $\Delta 70$, $\Delta 102$ FasL, and Vc were transfected into various cell lines as indicated. FasL cell surface expression by stable transfectants was detected by flow cytometric analysis using PE-A1F-2.1 anti-FasL mAb. The number in each panel indicates the percentage of cells expressing cell surface FasL. Values below 1.5% are considered undetectable based on staining with isotype-matched control mAb (data not shown).

FIGURE 2. WT, $\Delta 33$, and $\Delta 70$ FasL transfectants express cell-mediated cytotoxicity. Cell-mediated cytotoxicity of various transfectants of Neuro-2a (*a*) and NIH-3T3 (*b*) were conducted using ^{51}Cr -labeled A20 B lymphoma cells (2×10^4) as target. Cytotoxicity assays and the determination of cytotoxicity (expressed as % specific Cr-release) were conducted as described in *Materials and Methods*.



B lymphoma cells as targets. We first examined our WT transfectants. FasL-mediated cytotoxicity was detected for each of the five cell lines (data not shown). We then determined the cell-mediated cytotoxicity of transfectants of various deletion mutants of the Neuro-2a and NIH-3T3 cell lines (Fig. 2). In both series, FasL-mediated cytotoxicity was detected in a dose-dependent manner for transfectants of WT, $\Delta 33$, and $\Delta 70$ FasL. Cytotoxicity was not detected for $\Delta 102$ FasL or Vc transfectants in similar conditions. Thus, cell-mediated cytotoxicity apparently correlated with FasL

cell surface expression. However, the cytotoxic potentials of WT, $\Delta 33$, and $\Delta 70$ transfectants did not correlate well with FasL cell surface expression levels. WT transfectants that expressed significantly lower surface FasL than $\Delta 33$ or $\Delta 70$ FasL transfectants displayed cytotoxicity that is either similar to (in the case of Neuro-2a) or slightly stronger than (in the case of NIH-3T3) $\Delta 33$ and $\Delta 70$ FasL transfectants. The data strongly suggest that FasL_{Cy1} can influence FasL bioactivity across a membrane barrier (S. Jodo and S.-T. Ju, manuscript in preparation).

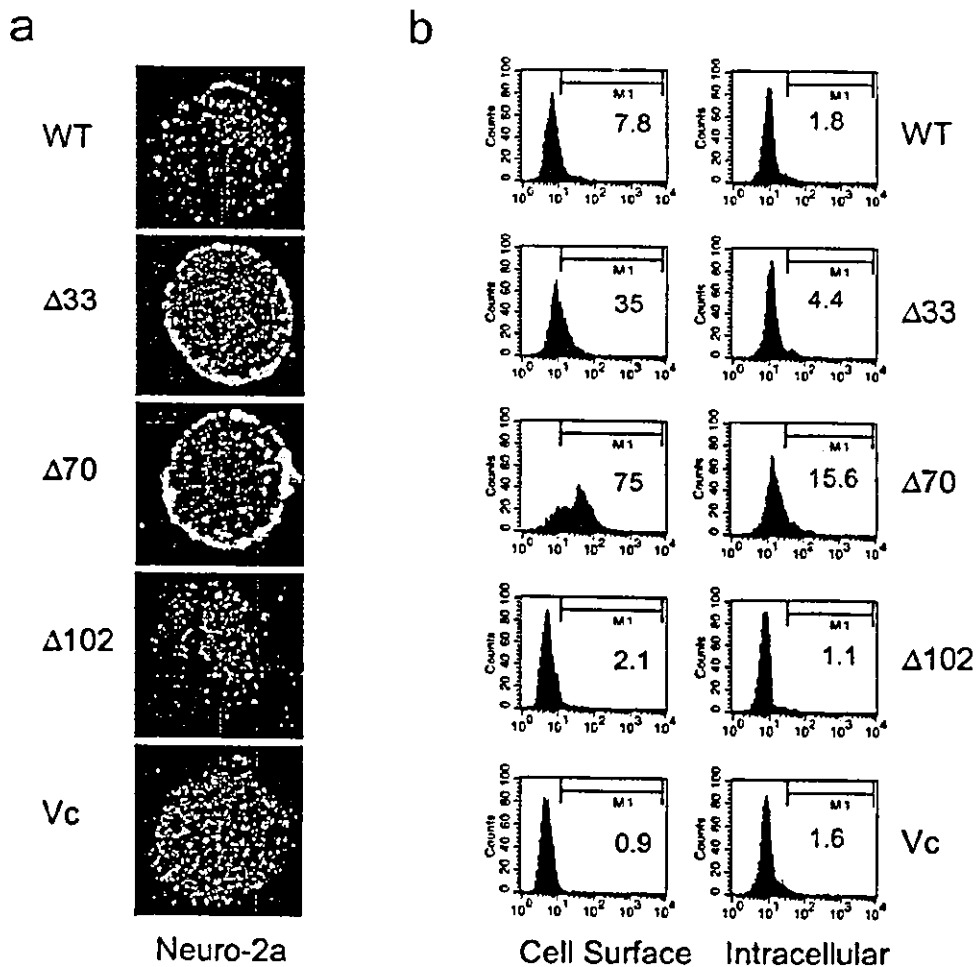


FIGURE 3. Expression of intracellular and cell surface FasL by various transfectants. *a*, Confocal microscopic analysis of intracellular and cell surface FasL. Stable transfectants of Neuro-2a cells were stained with FITC-NOK-1 mAb for cell surface expression of FasL, fixed, permeated, and then stained with PE-NOK-1 mAb for intracellular FasL expression. *b*, Cells were analyzed with a flow cytometer.

Effect of FasL_{Cyt} deletion on total FasL level

The observation that Δ33 FasL transfectants strongly expressed membrane FasL in five different cell lines demonstrated that FasL₂₋₃₃ was a negative regulator of FasL membrane expression. In addition, it was dominant over FasL_{PRD} because FasL membrane expression was increased even in the presence of intact FasL_{PRD} as observed in Δ33 FasL transfectants. Previous studies concluded that FasL_{PRD} prevents FasL from being expressed on the cell surface by retaining FasL in the secretory lysosomes (41). Because WT transfectants expressed low levels of cell surface FasL in our study, the possibility that FasL was retained inside the cells was addressed. For this purpose, FasL distribution at the cell surface and in the cytoplasm was determined using both confocal microscopy and flow cytometry. Confocal microscopic analysis showed that Δ33 FasL and Δ70 FasL transfectants of Neuro-2a cells have more cell surface and intracellular FasL than WT FasL transfectants (Fig. 3*a*). Indeed, flow cytometric analysis showed that 7.8, 35, and 75% of WT, Δ33, and Δ70 FasL transfectants, respectively, express cell surface FasL (Fig. 3*b*). Similarly, analysis on permeated cells indicated that Δ33 and Δ70 FasL transfectants have more intracellular FasL (4.4% for Δ33 and 15.6% for Δ70) than WT FasL transfectants (1.8%). In both analyses, FasL was not detected in Vc or Δ102 FasL transfectants. These data indicate that FasL_{Cyt} can negatively regulate FasL expression and that the PRD-containing transfectants (WT and Δ33) did not retain FasL in the cytoplasm. The total amount of FasL and its cell surface expression were both increased as a result of deletion of these regulators.

Determine the absolute FasL expression level of various transfectants

To provide quantitative determination on the effect of FasL_{Cyt} on total FasL expression levels, the total FasL levels of Neuro-2a and NIH-3T3 transfectants were measured using FasL-specific ELISA (Table I). For Neuro-2a transfectants, deleting FasL₂₋₃₃ resulted in a significant increase in FasL expression compared with WT FasL transfectant. Further deleting the FasL₃₄₋₇₀ segment caused more expression of total FasL. For NIH-3T3 transfectants, deleting FasL₂₋₃₃ also significantly increased total FasL level. However, only a modest increase in FasL expression was observed with the Δ70 FasL transfectant. As with confocal microscopic and flow cytometric analyses, ELISA measurements did not detect FasL expression in Vc or Δ102 FasL transfectants.

Mechanism of action of the FasL_{Cyt} negative regulator on FasL expression

Because FasL_{Cyt} did not retain FasL in the cytoplasm and the cell membrane FasL expression was proportional to total FasL levels of transfectants, we asked whether FasL expression was controlled at the transcriptional and/or translational levels. We used both RT-

PCR (Neuro-2a and RBL) and RNase protection assays (Neuro-2a and NIH-3T3) to determine the FasL transcription efficiencies of the various transfectants (Fig. 4). No significant differences in FasL-specific RT-PCR products were observed for any of the transfectants except Vc, which lacked FasL mRNA (Fig. 4*a*). Likewise, protected FasL mRNA was detected in all transfectants except Vc. The levels of protected FasL mRNA among various FasL transfectants of Neuro-2a and NIH-3T3 were similar (Fig. 4*b*). The data suggest that the increase in FasL expression levels was not caused by transcription efficiency differences.

The FasL translation efficiencies of our transfectants were determined by using [³⁵S]methionine labeling that detects the de novo synthesis of FasL. First, we conducted a 16-h labeling experiment in

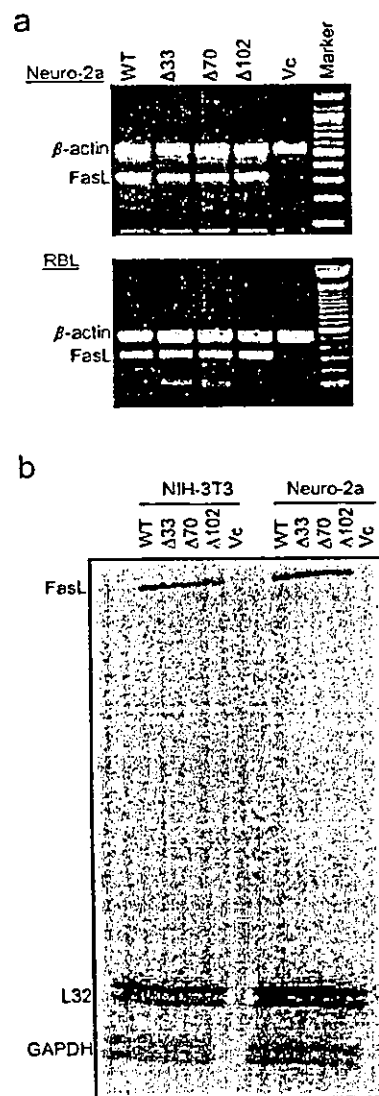


FIGURE 4. Transcription efficiency of FasL of various transfectants. *a*, Total RNA was isolated from various transfectants of Neuro-2a and RBL cells. FasL and control β-actin mRNA were measured by RT-PCR as described in *Materials and Methods*. The sizes of the PCR products are ~300 and 540 bp for FasL and β-actin, respectively. *b*, Total RNA was isolated from various transfectants of Neuro-2a and NIH-3T3 cells. FasL mRNA was measured by RNase protection assay using a customized kit. In this assay, a 3' fragment of FasL mRNA (encoding a FasL_{Cyt} fragment) was protected. The sizes of protected human FasL, mouse L32, and mouse GAPDH mRNA are 351, 112, and 97 bp, respectively.

Table I. FasL production by various transfected cell lines^a

| Cell Line | WT | Δ33 | Δ70 | Δ102 | Vc |
|-----------|-----|------|------|------|------|
| Neuro-2a | 1.7 | 12 | 32.3 | 0.2 | -0.2 |
| NIH-3T3 | 1.6 | 12.6 | 19.6 | -0.2 | 0 |

^a The results expressed in picomoles/sample are representative of two independent assays. Samples were prepared as described in *Materials and Methods* and determined for FasL amounts using FasL-specific ELISA kit (Oncogene). Standard curve was established with recombinant soluble FasL provided with the kit. The molecular mass of WT FasL used for calculation is 40,000 Da. The molecular mass of deletion mutants was calculated by subtracting the calculated molecular mass of the deleted amino acid residues from the molecular mass of the WT FasL.

Neuro-2a transfectants to determine whether the expression of labeled FasL correlated with FasL expression determined in earlier experiments. In this case, a very strong expression was observed with the $\Delta 70$ FasL transfectant, a strong expression was observed with the $\Delta 33$ FasL transfectant and a weak expression was observed with the WT transfectant (Fig. 5a, upper panel). The specificity of the assay system was demonstrated by the expected sizes of labeled FasL and by the fact that no detectable incorporation of [³⁵S]methionine into FasL was observed for the $\Delta 102$ FasL or Vc transfectant. This expression hierarchy was similar to that described earlier using flow cytometric and ELISA measurements. In addition, incorpo-

ration of [³⁵S]methionine into snRNP, a normal constituent of Neuro-2a cells, was comparable among transfectants (lower panel). These data indicate that the 16-h [³⁵S]methionine labeling experiment detects the homeostatic state of FasL expression.

To determine whether FasL_{C₃₁} regulates the rate of FasL de novo synthesis, we conducted short-term (5- or 10-min) [³⁵S]methionine labeling experiments in the COS-7 transfectants of WT, $\Delta 33$, and $\Delta 70$ FasL (Fig. 5b). In both cases, the amount of labeled FasL as measured by autoradiography correlated with FasL total expression levels determined in earlier experiments using flow cytometry and ELISA. The incorporation of [³⁵S]methionine into FasL in both the $\Delta 33$ and the $\Delta 70$ FasL transfectants was significantly higher than that in the WT FasL transfectant. A slightly higher level of [³⁵S]methionine-labeled FasL was observed in the $\Delta 70$ FasL transfectant than the $\Delta 33$ FasL transfectant (Fig. 5b, upper panel). The experiment determined the rate of de novo protein synthesis because a clear increase in [³⁵S]methionine incorporation was observed between 5- and 10-min labeling, and this increase was observed for both the transfected FasL and the control snRNP (Fig. 5b, lower panel). This increase in translation was specific because the de novo synthesis of snRNP proteins, under both the short-term (5- and 10-min) and the long-term (16-h) labeling conditions, was comparable among the transfectants. We also noted that the patterns for WT, $\Delta 33$, and $\Delta 70$ FasL were the same for COS-7 and Neuro-2a cells but the snRNP patterns were somewhat different (Fig. 5b). The results indicate that the increase in $\Delta 33$ and $\Delta 70$ FasL was due to an increase in the rate of de novo synthesis of the $\Delta 33$ and $\Delta 70$ FasL deletion mutants.

Discussion

Numerous specific motifs that target proteins to certain organelles have been identified. Motifs that regulate the total amount of transmembrane proteins have been described in a number of cases (44). The present study demonstrates that FasL_{C₃₁} regulates the total level as well as the cell surface expression of FasL. We have identified FasL₂₋₃₃ as a negative regulator of FasL expression. Presence of this region in FasL prevented strong expression of FasL. Deletion of FasL₂₋₃₃ increased both the total FasL expression and the membrane FasL expression. The observation of this activity in five cell lines of distinct origin indicated that this regulator functions in a cell type-independent manner. Based on the results obtained from $\Delta 70$ transfectants, FasL₃₄₋₇₀ also appears to negatively regulate FasL level. FasL₃₄₋₇₀ contained the PRD that has been shown to negatively regulate cell surface expression of GFP-FasL by retaining FasL in the secretory lysosomes (40, 41). However, our data indicated that the increase in FasL cell surface expression was mainly caused by the increase in total FasL expression. In addition, we demonstrated that FasL_{C₃₁} regulates FasL expression by limiting the rate of de novo synthesis of FasL.

There are two major differences between our findings and those described previously (27, 28). First, we have identified FasL₂₋₃₃ as the major negative regulator for FasL membrane expression, whereas Bossi and Griffiths (40, 41) reported that FasL₁₋₃₇ does not have a role in regulating FasL membrane expression. We observed that WT transfectants, irrespective of their cell types, express low levels of FasL unless FasL₂₋₃₃ or FasL₂₋₇₀ were deleted. In contrast, they reported high levels of GFP-FasL expression by WT transfectants that lack secretory lysosomes (40, 41). The second major difference was that we did not detect cytoplasmic retention of WT FasL. This was demonstrated by the low FasL levels in five distinct WT transfectants, irrespective of cell types or of whether they contained secretory lysosomes. In addition, confocal and fluorescent staining failed to reveal a strong retention of WT FasL in the cytoplasm.

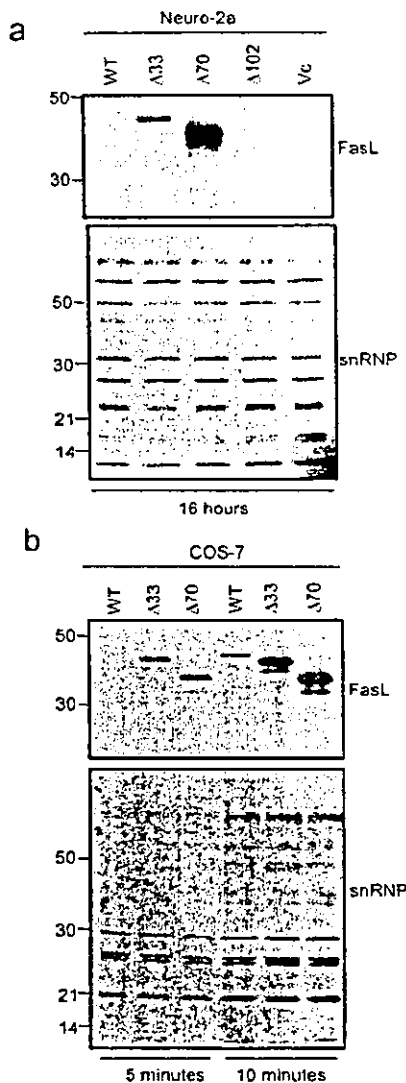


FIGURE 5. Translational regulation of FasL expression in various transfectants. *a*, Determination of the homeostatic expression of FasL based on long-term [³⁵S]methionine incorporation. Various FasL transfectants of Neuro-2a cells were cultured in labeling medium containing [³⁵S]methionine for 16 h. Labeled FasL and labeled snRNP were detected as described in *Materials and Methods*. The multiple bands of snRNP are due to the snRNP complex formed by various snRNP components. *b*, Determination of the de novo synthesis rate of FasL. Various FasL transfectants of COS-7 cells (WT, $\Delta 33$, and $\Delta 70$) were cultured in [³⁵S]methionine-containing labeling medium for 5 and 10 min, respectively. Labeled FasL and labeled snRNP were detected as described in *Materials and Methods*. The positions of m.w. standards are indicated on the left side of the gel.

There are several possible explanations for these discrepancies. First, Bossi and Griffiths (41) fused GFP to the N terminus of WT FasL and its deletion mutants. This could have modified the function of the N-terminal region of FasL. Because of the close proximity of GFP to the region examined and because of the large size of GFP relative to the small FasL_{C_{yt}}, functions such as regulation of FasL translation efficiency or FasL trafficking could have been affected. Our observations support the former possibility. In contrast, GFP fused in close proximity to PRD (position 37) apparently did not inhibit the regulatory function of FasL_{PRD} in their studies (40, 41). Second, we conducted all of our experiments with stable transfectants. Transient transfection used in their experiments may not permit sufficient time for the full execution of the regulatory mechanisms for FasL expression. In addition, transient transfection may not be influenced by FasL-mediated deletion of Fas⁺ transfectants. Third, the *fasl* gene used in their study had a leucine codon instead of cysteine in position 32. The amino acid they reported is different from those published in the literature (26) and those reported in the databanks. The importance of Cys³² residue was suggested by its conservation among humans, mice, and rats (39), and its potential involvement in acetylation, palmitoylation, or disulfide bonding. Fourth, Bossi and Griffiths deleted FasL₁₋₃₇ and we deleted FasL₂₋₃₃ (41). It is possible that FasL₃₃₋₃₇ contained the critical amino acids responsible for the observed difference. Finally, it is important to emphasize the dominant role of FasL₂₋₃₃ over FasL₃₃₋₇₀ (that contains the PRD) in mediating FasL expression in the present study. This dominance could have been lost in GFP-fused FasL. In support of this, we have generated ΔPRD FasL transfectants for NIH-3T3, Neuro-2a, and COS-7 cells, and increases in cell surface FasL expression on the transfectants were not observed (V. Pidiyar and S.-T. Ju, unpublished observation).

Regulation of FasL expression has been extensively studied in T cells. Activated T cells produce FasL as a result of increased *fasl* gene activation. Despite the inhibitory effect of FasL_{C_{yt}} negative regulatory elements implicated by the present study, activated T cells express FasL on the cell surface. Activation of T cells may induce other mechanisms that overcome the negative regulation by FasL_{C_{yt}}. One of the proposed mechanisms is based on activation-induced increases in secretory vesicle trafficking (45). However, activated T cells from *Ashen* mice that have a defect in activation-dependent lysosomal secretion were shown to express normal levels of FasL-mediated cytotoxicity (46). It is important to note that our findings are entirely consistent with the FasL expression on activated T cells because we demonstrated that the cell surface expression of FasL was directly proportional to the total FasL produced by cells and that WT FasL was not retained in the cytoplasm.

Our study suggests that the increase in FasL cell surface expression was mostly due to the increase in total FasL levels. Further analyses suggest that the FasL expression level, controlled by FasL₂₋₃₃, was not due to differences in transcription because all of the transfectants expressed comparable levels of FasL mRNA. This observation also indicated that the difference in FasL protein expression was not due to differences in transfection efficiency. The identical pattern of FasL expression by transfectants in both short- and long-term labeling experiments indicated that de novo synthesis of FasL was the major mechanism responsible for increased FasL expression in Δ33 and Δ70 transfectants (Fig. 5). As Δ33 and Δ70 contain, respectively, 90 and 75% of the amino acids of the WT FasL protein, the increase in the de novo synthesized FasL deletion mutants cannot be accounted for by their shortened peptide lengths. Other translational mechanisms must be responsible for the increase in total FasL expression.

Sequences of "short, nearly exact matches" to human FasL₁₋₇₀ based on "blast hits" were not found in any other transmembrane proteins in the protein databank of NCBI (www.ncbi.nlm.nih.gov). Our data suggest FasL₂₋₇₀ contains motifs that regulate FasL's translation rate. FasL is a type II transmembrane protein and FasL_{C_{yt}} contains three positively charged residues, K72K73R74, near its transmembrane domain (Fig. 1a). Because translocation of de novo synthesized transmembrane proteins is regulated by charged amino acids near the transmembrane domain (internal start-transfer sequence), it is likely that these positively charged amino acids are important for the translocation of nascent FasL chains through the endoplasmic reticulum (ER) membrane during de novo protein synthesis (47). The remarkable increase in FasL de novo synthesis resulting from the deletion of FasL₂₋₇₀ suggests that this early event of FasL translation is a rate-limiting step for FasL synthesis.

Deletion of FasL₂₋₃₃ also increased the rate of de novo synthesis of FasL. FasL₂₋₃₃ contains the sequence S17S18A19S20S21 and SXXS is a casein kinase I (CKI)-targeted motif. It has been suggested that this motif may provide a retrograde signaling during T cell activation (48). We have tested this motif for its ability to regulate total FasL expression and FasL cell surface expression. The CKI-specific inhibitor, CK-7 (49), used at optimal but nontoxic concentration, failed to exert a detectable effect on FasL expression by FasL WT transfectants of NIH-3T3 cells. Furthermore, no effect was observed with NIH-3T3 cells transfected with a mutant construct in which the S17S18A19S20S21 site was changed to AAAAA by site-directed mutagenesis (data not shown). These results provide strong evidence that the putative CKI motif in FasL₂₋₃₃ was not responsible for the regulation of FasL expression levels. FasL₂₋₃₃ also may have "dityrosine" motifs (Y7PY9PQIY13W, see Fig. 1a). Such dityrosine (YQ, YF) motifs in the CD3γ-chain have been implicated in ER retention and their presence results in reduced membrane expression (44). Perhaps, by regulating both ER translocation and ER retention, FasL_{C_{yt}} could effectively control FasL translation rates and ultimately total FasL expression levels, including expression on the plasma membrane. Study is in progress using more refined deletion mutants and using alanine-based substitution mutants in a systematic manner to identify the critical amino acid residue(s) responsible for the negative regulatory function of FasL_{C_{yt}}.

References

- Yonehara, S., A. Ishii, and M. Yonehara. 1989. A cell-killing monoclonal antibody (anti-Fas) to a cell surface antigen co-downregulated with the receptor of tumor necrosis factor. *J. Exp. Med.* 169:1747.
- Trauth, B. C., C. Klas, M. J. Peters, S. Matzku, P. W. Falk, K. M. Debatin, and P. H. Kramer. 1989. Monoclonal antibody-mediated tumor regression by induction of apoptosis. *Science* 245:301.
- Watanabe-Fukunaga, R., C. I. Brannan, N. G. Copeland, N. A. Jenkins, and S. Nagata. 1992. Lymphoproliferative disorder in mice explained by defects in Fas antigen that mediate apoptosis. *Nature* 356:314.
- Locksley, R., N. Killeen, and M. J. Lenardo. 2001. The TNF and TNF receptor superfamilies: integrating mammalian biology. *Cell* 104:487.
- Takahashi, T., M. Tanaka, C. I. Brannan, N. A. Jenkins, N. G. Copeland, T. Suda, and S. Nagata. 1994. Generalized lymphoproliferative disease in mice, caused by a point mutation in the Fas ligand. *Cell* 76:969.
- Lynch, D. H., M. L. Watson, M. L. Alderson, P. R. Baum, R. E. Miller, T. Tough, M. Gibson, T. Davis-Smith, C. A. Smith, K. Hunter, et al. 1994. The mouse Fas-ligand is mutated in the *gld* mice and is part of a TNF family gene cluster. *Immunity* 1:131.
- Rouvier, E., M.-F. Luciano, and P. Golstein. 1993. Fas involvement in Ca²⁺-independent T cell-mediated cytotoxicity. *J. Exp. Med.* 177:195.
- Ju, S.-T., H. Cui, D. J. Panka, R. Eitinger, and A. Marshak-Rothstein. 1994. Participation of target Fas protein in apoptosis pathway induced by CD4⁺ Th1 and CD8⁺ cytotoxic T cells. *Proc. Natl. Acad. Sci. USA* 91:4185.
- Stalder, T., S. Hahn, and P. Erb. 1994. Fas antigen is the major target molecule for CD4⁺ T cell-mediated cytotoxicity. *J. Immunol.* 152:1127.
- Ozdemirli, M., M. el-Khatib, L. C. Foote, J. K. M. Wang, A. Marshak-Rothstein, T. L. Rothstein, and S.-T. Ju. 1996. Fas (CD95)/FasL interactions regulate antigen-specific, MHC-restricted T/B cell proliferative responses. *Eur. J. Immunol.* 26:415.

11. Wu, J., T. Xhou, J. He, and J. D. Mountz. 1993. Autoimmune disease in mice due to integration of an endogenous retrovirus in an apoptosis gene. *J. Exp. Med.* 178:461.
12. Chu, J. L., J. Drappa, A. Parnassa, and K. B. Elkon. 1993. The defect in Fas mRNA expression in MRL/lpr mice is associated with insertion of the retrotransposon. *Etn. J. Exp. Med.* 178:723.
13. Adachi, M., R. Watanabe-Fukunaga, and S. Nagata. 1993. Aberrant transcription caused by the insertion of an early transposable element in an Intron of the Fas antigen gene of lpr mice. *Proc. Natl. Acad. Sci. USA* 90:1756.
14. Ju, S.-T., D. J. Panka, H. Cui, R. Ettinger, M. el-Khatib, D. H. Sherr, B. Z. Stanger, and A. Marshak-Rothstein. 1995. Fas (CD95)/FasL interactions required for programmed cell death after T cell activation. *Nature* 373:444.
15. Pinkoski, M. J., N. M. Droin, T. Lin, L. Genestier, T. A. Ferguson, and D. R. Green. 2002. Nonlymphoid Fas ligand in peptide-induced peripheral lymphocyte deletion. *Proc. Natl. Acad. Sci. USA* 99:16174.
16. Allison, J., H. M. Georgiou, A. Strasser, and D. L. Vaux. 1997. Transgenic expression of CD95 ligand on islet β cells induces a granulocytic infiltration but does not confer immune privilege upon islet allografts. *Proc. Natl. Acad. Sci. USA* 94:3943.
17. Arai, H., D. Gordon, E. G. Nabel, and G. J. Nabel. 1997. Gene transfer of Fas ligand induces tumor regression in vivo. *Proc. Natl. Acad. Sci. USA* 94:13862.
18. Hohlbaum, A., M. S. Moe, and A. Marshak-Rothstein. 2000. Opposing effects of transmembrane and soluble Fas-ligand on inflammation and tumor cell survival. *J. Exp. Med.* 191:1209.
19. Hill, L. L., A. Ouhaiti, S. M. Loughlin, M. Kripke, H. N. Ananthaswamy, and L. N. Owen-Schaub. 1999. Fas ligand: a sensor for DNA damage critical in skin cancer etiology. *Science* 285:898.
20. Wei, Y., K. Chen, G. C. Sharp, H. Yagita, and H. Braley-Mullen. 2001. Expression and regulation of Fas and Fas ligand on thymocytes and infiltrating cells during induction and resolution of granulomatous experimental autoimmune thyroiditis. *J. Immunol.* 167:6678.
21. Borgerson, K. L., J. D. Bretz, and J. R. Baker, Jr. 1999. The role of Fas-mediated apoptosis in thyroid autoimmune disease. *Autoimmunity* 30:251.
22. Xiao, S., S.-s. J. Sung, S. M. Fu, and S.-T. Ju. 2003. Combining Fas mutation with IL-2 deficiency prevents both colitis and lupus. *J. Biol. Chem.* 278:52730.
23. Hohlbaum, A. M., M. S. Gregory, S.-T. Ju, and A. Marshak-Rothstein. 2001. Fas ligand engagement of resident peritoneal macrophages in vivo induces apoptosis and the production of neutrophil chemotactic factors. *J. Immunol.* 167:6217.
24. Bellgrau, D., and R. C. Duke. 1999. Apoptosis and CD95 ligand in immune privileged sites. *Int. Rev. Immunol.* 18:547.
25. Griffith, T. S., X. Yu, J. M. Hemdon, D. R. Green, and T. A. Ferguson. 1996. CD95-induced apoptosis of lymphocytes in an immune privileged site induces immunological tolerance. *Immunity* 5:7.
26. Matsui, K., A. Fine, B. Zhu, A. Marshak-Rothstein, and S.-T. Ju. 1998. Identification of two NF- κ B sites in mouse CD95 ligand (Fas ligand) promoter: functional analysis in T cell hybridoma. *J. Immunol.* 161:3469.
27. Latinis, K. M., L. L. Carr, E. J. Peterson, L. A. Norian, S. K. Eliason, and G. Koretzky. 1997. Regulation of CD95 (Fas) ligand expression by TCR-mediated signaling events. *J. Immunol.* 158:4602.
28. Matsui, K., S. Xiao, A. Fine, and S.-T. Ju. 2000. Role of activator protein-1 in TCR-mediated regulation of murine *fasl* promoter. *J. Immunol.* 164:3002.
29. Xiao, S., K. Matsui, A. Fine, and S.-T. Ju. 1999. FasL promoter activation by IL-2 through SP1 and NFAT but not Egr-2 and Egr-3. *Eur. J. Immunol.* 29:3456.
30. Mittelstadt, P. R., and J. D. Ashwell. 1998. Cyclosporin A-sensitive transcription factor Egr-3 regulates Fas ligand expression. *Mol. Cell. Biol.* 18:3744.
31. Holtz-Heppelmann, C. J., A. Algeciras, A. D. Badley, and C. V. Paya. 1998. Transcriptional regulation of the human FasL promoter-enhancer region. *J. Biol. Chem.* 273:4416.
32. Wu, J., C. Metz, X. Xu, R. Abe, A. W. Gibson, J. C. Edberg, J. Cooke, F. Xie, G. S. Cooper, and R. P. Kimberly. 2003. A novel polymorphic CAAT/enhancer-binding protein β element in the FasL gene promoter alters Fas ligand expression: a candidate background gene in African American systemic lupus erythematosus patients. *J. Immunol.* 170:132.
33. Mor, G., E. Sapi, V. M. Abrahams, T. Rutherford, J. Song, X. Y. Hao, S. Muzaffar, and F. Kohen. 2003. Interaction of the estrogen receptors with the Fas ligand promoter in human monocytes. *J. Immunol.* 170:114.
34. Schneider, P., N. Holler, J.-L. Bodmer, M. Hahne, K. Frei, A. Fontana, and J. Tschopp. 1998. Conversion of membrane bound Fas (CD95) ligand to its soluble form is associated with downregulation of its proapoptotic activity and loss of liver toxicity. *J. Exp. Med.* 187:1205.
35. Tanaka, M., T. Imai, M. Adachi, and S. Nagata. 1998. Down-regulation of Fas ligand by shedding. *Nat. Med.* 4:31.
36. Martinez-Lorenzo, M. J., A. Anel, S. Gamen, I. Monleon, P. Lasierria, L. Larrad, A. Pinerio, M. A. Alava, and J. Naval. 1999. Activated human T cells release bioactive Fas ligand and APO2 ligand in microvesicles. *J. Immunol.* 163:1274.
37. Strelow, D., S. Jodo, and S.-T. Ju. 2000. Retroviral membrane display of apoptotic effector molecules. *Proc. Natl. Acad. Sci. USA* 97:4209.
38. Jodo, S., S. Xiao, A. Hohlbaum, D. Strelow, A. Marshak-Rothstein, and S.-T. Ju. 2001. Apoptosis-inducing membrane vesicles: a novel agent with unique properties. *J. Biol. Chem.* 276:39938.
39. Takahashi, T., M. Tanaka, J. Inazawa, T. Abe, T. Suda, and S. Nagata. 1994. Human Fas ligand: gene structure, chromosomal location and species specificity. *Int. Immunol.* 6:1567.
40. Bossi, G., and G. M. Griffiths. 1999. Degranulation plays an essential part in regulating cell surface expression of Fas ligand in T cells and natural killer cells. *Nat. Med.* 5:90.
41. Blott, E. J., G. Bossi, R. Clark, M. Zvelebil, and G. M. Griffiths. 2001. Sorting out the multiple roles of Fas ligand. *J. Cell Sci.* 114:2405.
42. Xiao, S., A. Marshak-Rothstein, and S.-T. Ju. 2001. Sp1 is the major *fasl* gene activation in abnormal CD4⁺ D8 220⁺ T cells of lpr and gld mice. *Eur. J. Immunol.* 31:3339.
43. Deshmukh, U. S., and C. C. Kannappell, S. M. Fu. 2002. Immune responses to small nuclear ribonucleoproteins: antigen-dependent distinct B cell epitope spreading patterns in mice immunized with recombinant polypeptides of small nuclear ribonucleoproteins. *J. Immunol.* 168:5326.
44. Letourmeur, F., and R. D. Klausner. 1992. A novel di-leucine motif and a tyrosine-based motif independently mediate lysosomal targeting and endocytosis of CD3 chains. *Cell* 69:1143.
45. Blott, E. J., and G. M. Griffiths. 2002. Secretory lysosomes. *Nat. Rev. Mol. Cell Biol.* 3:122.
46. Haddad, E. K., X. Wu, J. A. Hammer, and P. A. Henkart. 2001. Defective granule exocytosis in Rab27a-deficient lymphocytes from *Ashen* mice. *J. Cell Biol.* 152:835.
47. Gerace, L., R. Gilmore, A. Johnson, P. Lazacow, W. Neupert, E. O'Shea, and K. Weis. 2002. Intracellular compartments and protein sorting. In *Molecular Biology of the Cell*, 4th ed. B. Alberts, A. Johnson, J. Lewis, M. Raff, K. Roberts, and P. Walter, eds. Garland Science, New York, p. 659.
48. Watts, A. D., N. H. Hunt, Y. Wanigasekara, G. Bloomfield, D. Wallach, B. D. Roufogalis, and G. Chaudhri. 1999. A casein kinase I motif present in the cytoplasmic domain of members of the tumour necrosis factor ligand family is implicated in "reverse signaling". *EMBO J.* 18:2119.
49. Chijiga, T., M. Hagiwara, and H. Kidaka. 1989. A newly synthesized selective casein kinase I inhibitor, N-(2-aminoethyl)-5-chloroisquinoline-8-sulfonamide, and affinity purification of casein kinase I from bovine testis. *J. Biol. Chem.* 264:4924.



β_2 -glycoprotein I, anti- β_2 -glycoprotein I, and fibrinolysis

Shinsuke Yasuda*, Tatsuya Atsumi, Masahiro Ieko, Takao Koike

Department of Medicine II, Hokkaido University Graduate School of Medicine, N15 W7, Kita-ku,
Sapporo 060-8638, Japan

Received 10 June 2004; received in revised form 25 July 2004; accepted 29 July 2004
Available online 9 September 2004

KEYWORDS

β_2 GPI;
Fibrinolysis;
Natural anticoagulant
regulator

Abstract β_2 -glycoprotein-I (β_2 GPI) is a phospholipid-binding plasma protein that consists of five homologous domains. Domain V is distinguished from others by bearing a positively charged lysine cluster and hydrophobic extra C-terminal loop. β_2 GPI has been known as a natural anticoagulant regulator. β_2 GPI exerts anticoagulant activity by inhibition of phospholipid-dependent coagulation reactions such as prothrombinase, tenase, and factor XII activation. It also binds factor XI and inhibits its activation. On the other hand, β_2 GPI inhibits anticoagulant activity of activated protein C. According to the data from knockout mice, β_2 GPI may contribute to thrombin generation in vivo. Phospholipid-bound β_2 GPI is one of the major target antigens for antiphospholipid antibodies present in patients with antiphospholipid syndrome (APS). Binding of pathogenic anti- β_2 GPI antibodies increases the affinity of β_2 GPI to the cell surface and disrupts the coagulation/fibrinolysis balance on the cell surface. These pathogenic antibodies activate endothelial cells via signal transduction events in the presence of β_2 GPI. Impaired fibrinolysis has been reported in patients with APS. Using a newly developed chromogenic assay, we demonstrated lower activity of intrinsic fibrinolysis in euglobulin fractions from APS patients. Addition of monoclonal anti- β_2 GPI antibodies with β_2 GPI also decreased fibrinolytic activity in this assay system. β_2 GPI is proteolytically cleaved by plasmin in domain V (nicked β_2 GPI) and becomes unable to bind to phospholipids, reducing antigenicity against antiphospholipid antibodies. This cleavage occurs in patients with increased fibrinolysis turnover. Nicked β_2 GPI binds to plasminogen and suppresses plasmin generation in the presence of fibrin, plasminogen, and tissue plasminogen activator (tPA). Thus, nicked β_2 GPI plays a role in the extrinsic fibrinolysis via a negative feedback pathway loop. © 2004 Elsevier Ltd. All rights reserved.

* Corresponding author. Tel.: +81 11 706 5915; fax: +81 11 706 7710.
E-mail address: syasuda@med.hokudai.ac.jp (S. Yasuda).